Revealing the cryptic diversity of the hosts of Rio Mamoré orthohantavirus complex, *Oligoryzomys microtis* (Allen 1916) (Rodentia: Cricetidae: Sigmodontinae), with the description of one new species with two subspecies

Cibele Rodrigues Bonvicino[1], Marcelo Weksler[2]

[1]Instituto Oswaldo Cruz, FIOCRUZ
[2]Museu Nacional / UFRJ

Cibele Rodrigues Bonvicino - 0000-0002-1948-7643
Marcelo Weksler - 0000-0001-8111-4779

Short Title: Description of new species of *Oligoryzomys microtis* complex

Abstract

Oligoryzomys is a widespread and speciose genus of Neotropical rodents of the subfamily Sigmodontinae, including several species that are natural reservoirs of hantavirus and other zoonotic pathogens. Although Sigmodontinae species are generally considered to be species-specific reservoirs of *Orthohantavirus*, *Oligoryzomys microtis* is an exception, as it is the reservoir of four different genotypes of the Rio Mamoré orthohantavirus: RIOMV, HTN-007, RIOMV-3, and RIOMV-4. Here we demonstrate, based on comparative morphology, karyology, and phylogenetic analyses of the mitochondrial gene cytochrome *b* and the intron 7 of the β-fibrinogen nuclear gene, that *O. microtis* is a cryptic species complex with three geographically structured lineages and two different karyotypes. The lineages are parapatric, with one occurring in western Amazonia and north of the Amazonas-Solimões River, the second in transitional areas (ecotones) from central Amazonia with the Cerrado of central Brazil, and the third in eastern Amazonia south of Amazonas River. We establish that one lineage of *O. microtis* is the reservoir of the Rio Mamoré orthohantavirus genotypes RIOMV, HTN-007, and RIOMV-3 from Peru, Bolivia, and the Brazilian states of Amazonas and Acre. The second lineage is the reservoir of orthohantavirus Rio Mamoré genotype RIOMV-4 from the Brazilian state of Rondônia, whereas no orthohantavirus has been associated with the third lineage. The second and third lineages differ from *O. microtis sensu stricto* in chromosomal fundamental numbers (64 versus 66). The three lineages form monophyletic units in the cytochrome *b* tree, each supported by several synapomorphies. However, the three forms are morphologically very similar regarding external, cranial, and dental traits. Based on these karyological, molecular, and morphological results, we describe a new species of *Oligoryzomys* with two subspecies,

and discuss the implications of our taxonomic revision for the evolutionary history of Rio Mamoré orthohantavirus.

Key words: *Oligoryzomys*, new species, new subspecies, karyotype, morphology, molecular phylogeny

Introduction

With 26 recognized species, *Oligoryzomys* Bangs is a widespread and species-rich genus of Neotropical muroid rodents (Hurtado and D'Elía 2018, da Cruz et al. 2019, Hurtado 2021) distributed from Mexico to Tierra del Fuego (Weksler and Bonvicino 2015). Ten *Oligoryzomys* species are recognized as reservoirs for *Orthohantavirus* genotypes in the Neotropics, with five of them having been found to be orthohantavirus positive in Brazil: *O. flavescens*, *O. mattogrossae*, *O. microtis*, *O. nigripes*, *O. utiaritensis* (Suzuki *et al.* 2004, Rosa *et al*. 2005, Oliveira *et al.* 2009, Rosa *et al*. 2010, 2011, Oliveira *et al*. 2011, González-Ittig *et al.* 2014, Mull *et al.* 2020).

Several species of *Oligoryzomys* are well adapted to invasion of altered areas, such as agricultural and pasture landscapes, and zoonotic spillover happens due to the frequent peridomiciliary contact in areas of environmental destruction (Mull *et al.* 2020). One of the most important areas of zoonotic interest in South America is the agricultural frontier of central Brazil and northeastern Bolivia into Amazon, in which extensive transformation of rainforest into (especially) soybean monocultures and cattle have led to an extensive number of Hantavirus pulmonary syndrome (HPS) cases (Oliveira *et al.* 2014).

Oligoryzomys microtis Allen 1916, the reservoir of Rio Mamoré orthohantavirus (Oliveira et al. 2014), is the most widespread species in the Amazon basin, being found

in the Brazilian states of Acre, Amazonas, Mato Grosso, Rondônia and Pará, the Bolivian departments of Beni, Cochabamba, La Paz, Pando, and Santa Cruz, and the Peruvian departments of Amazonas, Loreto, Madre de Dios, Pasco, and Ucayali (Weksler and Bonvicino 2015). The role of *Oligoryzomys microtis* in the transmission of Rio Mamoré orthohantavirus and its variants is well documented (Oliveira *et al*. 2014). Rio Mamoré virus was first described in *O. microtis* from El Beni and La Paz departments in Bolivia (Bharadwaj *et al.* 1977), and posteriorly identified in *O. microtis* specimens from Santa Cruz department in Bolivia (Carroll *et al.* 2005), Loreto region in Peru (Powers *et al*. 1999, Richter *et al*. 2010), and Amazonas, Acre, and Rondônia states in Brazil (Firth *et al*. 2012, Nunes et al. 2015). Concomitantly, human cases were registered in Peru (Castillo *et al*. 2012, Casapía *et al*. 2012) and Brazil (Oliveira *et al*. 2014). Among all reported cases, four variants of Rio Mamoré orthohantavirus have been identified: RIOMV in Bolivia; HTN-007 in Peru; RIOMV-3 in Acre and Amazonas states, Brazil; and RIOMV-4 in Rondônia state, Brazil (Powers *et al*. 1999, Firth *et al*. 2012, Oliveira *et al.* 2014, Guterres et al. 2015).

The taxonomy of *Oligoryzomys* is hampered by a high level of morphological similarity among distinct phylogenetic lineages. Furthermore, due to the superficial similarities among the chromosome complements of several species, such as *O. microtis*, *O. mattogrossae* and *O. flavescens*, several mistaken associations between karyotypes and these species have been already produced (Weksler and Bonvicino 2015). Several currently recognized species have been considered as junior synonyms of *O. microtis*, such as *O. mattogrossae, O. fornesi*, and *O. utiaritensis*, (see Agrellos et al. 2012, Weksler et al. 2017). However, despite the resolution of these taxonomic issues, the last taxonomic checklist of *Oligoryzomys* still considered *O. microtis* as a putative species complex (Weksler and Bonvicino 2015), and several molecular analyses have indicated

phylogenetic structuring of geographically separated individuals within the species (Weksler et al. 2017, da Cruz and Weksler 2018, da Cruz et al. 2019, Hurtado and D'Elía 2019, 2022).

Given the importance of correct taxonomic identification of reservoirs for a complete understanding of orthohantavirus transmission cycles, and for assessing their potential as host transmitters of orthohantavirus to humans, we herein review the taxonomy of *Oligoryzomys microtis*, the reservoir of Rio Mamoré orthohantavirus and related virus. In particular, we analyze the anatomical, morphometric, cytogenetic, and molecular variability among a geographically wide sample of *Oligoryzomys microtis*, including the forms recognized as candidate species in previous molecular studies (e.g., *Oligoryzomys* sp. 1 and *Oligoryzomys* sp. 2 of Hurtado and D´Elía 2022), referred here as *Oligoryzomys* sp. n.

Material and methods

Morphological analysis

Oligoryzomys microtis specimens were collected from the type locality and several other Brazilian localities in Cerrado and Amazonas (Fig. 1, appendix 1). Collecting and permits were issued by SISBIO (System of Authorization and Information in Biodiversity) license numbers 13373 and 11375. The capture and handling of the specimens were under permission of the FIOCRUZ Ethics Committee (#1260/14) and followed the guidelines of the American Society of Mammalogists (Sikes et al. 2016). Animals were euthanized and voucher material and tissues were deposited in the mammal collections of Museu Nacional/UFRJ (MN) and LBCE (IOC/FIOCRUZ) (see appendix 1 for a list of specimens and locality information).

We examined additional *Oligoryzomys* specimens deposited in the mammals' collections of the following institutions: (1) MN - Museu Nacional, Universidade Federal do Rio de Janeiro, Rio de Janeiro, Brazil, (2) AMNH - American Museum of Natural History, New York, USA, including the type series of *O. utiaritensis*, *O. mattogrossae*, and *O. microtis*, (3) USNM - United States National Museum (Smithsonian Institution), Washington D.C., (4) LBCE - Laboratório de Biologia e Parasitologia de Mamíferos Reservatórios Silvestres, IOC-Fiocruz, Rio de Janeiro, Brazil (note that SVS - Secretaria de Vigilância em Saúde - specimens are housed at LBCE). Among the analyzed specimens, four were positive carriers of *Orthohantavirus* (see appendix 1) as reported by Nunes *et al.* (2015). Information on collection locality data (Fig. 1), museum acronyms and numbers are presented in appendix 1; see also Bonvicino and Weksler (1998), Weksler and Bonvicino (2005), Agrellos *et al*. (2012), and Weksler et al. (2017) for previously analyzed specimens of other *Oligoryzomys* species.

The terminology of characters herein analyzed follows previous studies (Reig 1977, Voss 1988, Carleton and Musser 1989, Weksler 2006). For color nomenclature, we followed Ridgway (1912) and Villalobos-Dominguez and Villalobos (1947). The following external dimensions were measured (in millimeters) in specimens collected by us, or obtained from original specimen tags: total length (ToL), head and body length (HBL), tail length (TL), ear length (Ear), hind foot length with claw (HF) and body mass (Wt). Whenever total length had been originally reported in specimen tags, HBL was estimated by subtracting tail length (TL) from total length. Cranial measurements were taken with digital calipers to the nearest 0.01 mm. For morphometric analyses, we employed 12 cranial dimensions following Bonvicino and Weksler (1998): condylo-incisive length (CIL), length of diastema (LD), palatal bridge (PB), length of maxillary molars (LM), breadth of first maxillary molar (BM1), external alveolar breadth (M1M),

length of incisive foramen (LIF), breadth of incisive foramen (BIF), rostrum breadth (BRO), orbital length (ORL), zygomatic breadth (ZB), and breadth of zygomatic plate (BZP). These dimensions were chosen because they provided consistent estimates by different investigators (*i.e*., did not display significant inter-researcher differences in paired *t* tests; data not shown).

Morphometric analyses of skull characters were performed for adult specimens, *i.e*., specimens with all teeth erupted and with at least minimal wear (Oliveira *et al*. 1998); males and females were grouped due to lack of sexual dimorphism (t-tests, $p<0.05$; data not shown). We computed descriptive statistics (average, standard deviation, minimum and maximum) and employed Analysis of Variance (ANOVA) with TUKEY *post hoc* test (Sokal and Rohlf 1994) and MANOVA, using logarithmic-transformed data to compare sets of populations of *O. microtis* from eastern, central and western Amazon (see map in fig. 1); the geographic limits of the population sets were also based on previous karyotypic and molecular data (Weksler et al. 2017, da Cruz and Weksler 2018, da Cruz et al. 2019, Hurtado and D'Elía 2019). We adjusted the individual measurements' alpha using Holm´s Sequential Bonferroni correction to reflect an overall alpha of 0.05 (Holm 1979, Rice 1989). We also employed principal component analysis and discriminant canonical analysis (Strauss 2010) to identify patterns of multivariate morphometric variation among the populations. Measurements were transformed to natural logs and covariance matrices were computed, considering all variables. All statistical analyses were performed in R version 4.0.2 using Rstudio (Rstudio Team 2020) using the MASS and candisc packages (Friendly and Fox 2010, Ripley et al. 2013). Because both PCA and DFA require complete data sets, missing values (2.1% of the total dataset) were estimated from the existing raw data using the missMDA package (Josse and Husson 2016) implemented in R.

Karyotype data and molecular phylogenetic analysis

We karyotyped eight specimens of *Oligoryzomys microtis* and 15 *Oligoryzomys* sp. n. (Table 1, appendix 1). Cell suspensions were obtained in the field with short-term bone marrow culture as previously reported (de Andrade *et al.* 2003). Chromosomes were ordered according to morphology and decreasing size, and fundamental numbers refer to the count of autosomal (i.e., non-sex) chromosomes.

DNA was isolated from livers preserved in 100% ethanol following the standard phenol-chloroform protocol (Sambrook and Russell 2001). The entire cytochrome *b* gene (mt-Cytb; gene acronym following *Mus musculus* nomenclature of Eppig *et al*. 2015) was amplified with primers L14724 (5'– CGAAGCTTGATATGAAAAACCATCGTTG – 3'; Irwin *et al*. 1991) and Citb-Rev (5'– GAATATCAGCTTTGGGTGTTGRTG –3'; Casado *et al*. 2010) by standard PCR procedures. Amplifications were performed in 50μL reactions with Platinum® Taq Polymerase (Invitrogen™) and recommended concentrations of primers and templates. Reactions were run for 35 cycles at 94°C for 30 s, 58°C for 30 s, and extension at 72°C for 90 s, with initial denaturation at 94°C for 2 min and final extension at 72°C for 7 min. Amplicons were purified either with GFX® PCR DNA or Gel Band Purification Kit (GE™ Healthcare) and sequenced with the same primers used in the PCR amplification and additional internal primers for mt-Cytb: MEU1 (Bonvicino and Moreira 2001) and MVZ16 (Smith and Patton 1993). Sequencing reactions were run in an ABI3130*xl* (Applied Biosystems) platform and electropherograms were manually checked and aligned using BioEdit 8.0 (Hall 1999) and Chromas 1.45 (McCarthy 1998).

We also amplified the intron 7 of the nuclear β-fibrinogen gene (i7-Fgb) of six *O. microtis* specimens with the primer pair β17-mammL and βfib-mammU as reported by Matocq *et al.* (2007). Amplifications were performed with 30 cycles of denaturation at

94°C for 1 min, 60°C for 30 s, and extension at 72°C for 1 min, with an initial denaturation at 94°C for 5 min and final extension at 72°C for 7 min.

Additional mt-Cytb and i7-Fgb data from GenBank *Oligoryzomys* specimens were used for phylogenetic reconstructions (appendix 2). We also performed a combined analysis of mt-Cytb and i7-Fgb. For the combined analyses, we included only exemplars with both mt-Cytb and i7-Fgb, except for the outgroup *Hylaeamys megacephalus*, for which sequences of each gene are from different individuals (appendix 2). We employed nine oryzomyines and three non-oryzomyines sigmodontines as outgroup taxa (appendix 2) in all phylogenetic analyses, and rooted our trees using *Sigmodon hispidus*.

Maximum Likelihood (Felsenstein 1981) and Bayesian analyses (Huelsenbeck *et al.* 2001) were carried out for phylogenetic reconstructions. The nucleotide evolution model was selected using Akaike Information Criteria (AICc) as estimated by Paup* 4.0a146 (Swofford 2002; commands AutoModel modelset=j7). The GTR model of nucleotide substitution (Rodríguez *et al*. 1990), corrected for site-specific rate heterogeneity using gamma distribution with four classes (Yang 1994) and proportion of invariant sites, was used for mt-Cytb, while GTR+G was used for i7-Fgb. Concatenated analyses employed unlinked partitioned models. Maximum-likelihood trees were built with RaxML-NG (Kozlov et al. 2019) and nodal bootstrap values (Felsenstein 1985) were calculated using 1,000 pseudoreplicates. Bayesian analyses were performed using Markov chain Monte Carlo (MCMC) sampling as implemented in MrBayes 3.1.2 (Ronquist and Huelsenbeck 2003). Uniform interval priors were assumed for all parameters except base composition, for which we assumed a Dirichlet prior. We performed four independent runs of 10,000,000 generations each, with two heated chains sampling for trees and parameters every 10,000 generations. The first 10,000 generations

were discarded as burn-in, and the remaining trees were used to estimate posterior probabilities for each node. Independent runs were combined with LogCombiner (version 2.6.6; Drummond and Rambaut 2007). All analyses were checked for convergence by plotting the log-likelihood values against generation time for each run with Tracer 1.4 (Rambaut and Drummond 2007), and all parameters had an effective sample size (ESS) over 500. Phylogenetic analyses were run in the CIPRES Science Gateway (Miller *et al.* 2010).

The Median-Joining (MJ) network (Bandelt *et al*. 1999) based on partial mt-Cytb sequences (801 bp) was reconstructed in the Network program (version 4.5.1.6) to evaluate the spatial and populational structuring of haplotypes. We retained only variable sites, and excluded any sites with missing data. Only specimens with sequences $\geq$ 777 bp were included (Appendix 3). To assess the genetic distinctiveness of the lineages within *O. microtis* species group, we calculated uncorrected genetic distances (*'p'*) between individuals.

Results

Karyotype

Karyotypic analysis of 15 specimens of *Oligoryzomys* sp. n. from Rondônia, Mato Grosso, Mato Grosso do Sul, and Tocantins states showed the same karyotype, 2n=64 and FN=64 (Table 1, fig. 2B and 2D). The autosomal complement is composed of one small-sized biarmed chromosome, and 30 acrocentric pairs varying in size from large to small, plus a large-sized X chromosome. The karyotypic analysis of eight specimens of *O. microtis* from Acre and Amazonas states, including one topotype, showed 2n=64 and FN=66 (Table 1, fig. 2A). The autosome complement is composed of two biarmed chromosomes, one very large (the largest of the chromosome complement) and one small

sized, 29 pairs of acrocentric chromosomes, and a median sized X chromosome. These chromosomal complements have been previously reported in the literature (Table 1).

Phylogenetic analyses

The ML and BA analyses based on the mt-Cytb recovered similar topologies, the differences among them being restricted to clades with low support. Both analyses recovered the clade containing *O. microtis* and *Oligoryzomys* sp. n. in the most basal dichotomy within *Oligoryzomys*, while all other 23 species were recovered in a poorly supported sister clade (Fig. 3). Within the former clade, referred as *O. microtis* species group, two clades were recovered: one with specimens of *O. microtis sensu stricto*, from Peru, Bolivia, and the Brazilian states of Acre and Amazonas (western Amazon), including the topotype specimen MN84349; and the second with specimens of *Oligoryzomys* sp. n. from Tocantins, Mato Grosso and Rondônia states. This clade is further separated in two well supported subclades, structured geographically into samples from Mato Grosso and Rondônia in one side (south central Amazon, referred as Central clade), and samples from Tocantins (southeastern Amazon, referred as Eastern clade) in another clade.

Combined analyses of mt-Cytb and i7-Fgb recovered the monophyly of *Oligoryzomys*, which was sister group of *Neacomys* (sup. fig. 1). The ML and BI analyses converged in similar topologies, but the BI is less fully resolved, and disagreements are centered on poorly supported relationships. The first dichotomy within *Oligoryzomys* separates a clade containing *O. microtis* species group and *O. mattogrossae* from a clade containing the remaining 20 species; *O. microtis* is recovered with a deep split separating specimens from western amazon (MVZ193858 from Amazonas state in Brazil and MUSM21846 from Madre de Dios in Peru) from samples from central (MN91804 from

Rondônia) and eastern (MN81639 from Tocantins) Amazon. Remaining *Oligoryzomys* species are further divided into two subclades, but with lower support. Six clades have high levels of support: 1: (*O. stramineus* + *O. nigripes*); 2: (*O. moojeni* + *O. rupestris*); 3: (*O. messorius*, (*O. delicatus*, (*O. costaricensis*, (*O. vegetus* + *O. fulvescens*)))), with *O. utiaritensis* as sister group with low support; 4: ((*O. occidentalis* + *O. longicaudatus*), (*O. fornesi* + *O. flavescens*)), the latter species not recovered monophyletic; 5: (*O. chacoensis*, *O. destructor*); and 6: ((*O. arenalis* + *O. guille*), *O. andinus*), the latter species not recovered monophyletic.

The median-joining network with mt-Cytb delineated three major haplogroups (Fig. 4A; appendix 3): the first corresponds to *O. microtis s.s.*, with specimens from Bolivia, Peru, and the Brazilian states of Amazonas and Acre; the second group included specimens of *Oligoryzomys* sp. n. from the Brazilian state of Rondônia (corresponding to the Central clade of the phylogenetic analyses), while the third included specimens from Tocantins (Eastern clade). The latter two haplogroups were separated by 35 mutations and four median vectors, but the first haplogroup was separated from the latter two by at 46 and 51 mutations and four median vectors. The first haplogroup was further divided into two subgroups, one with specimens from Peru and the Brazilian states of Amazonas and Acre separated by 11 nucleotide substitutions and two median vectors from the cluster with specimens from Bolivia and the Brazilian state of Acre. Genetic distances (uncorrected *p*, average, minimum and maximum) using mt-Cytb sequences were (Fig. 4B): 7.4% (6.8% - 8.3%) between *O. microtis* s.s. and *Oligoryzomys* sp. n. Eastern clade; 7.4% (6.3% - 9.5%) between *O. microtis* s.s. and *Oligoryzomys* sp. n. Central clade; and 5.4% (4.9% - 5.9%) between the central and Eastern clades of *Oligoryzomys* sp. n..

Morphology

Specimens belonging to the different lineages of the *O. microtis* species group exhibit very similar integumental, cranial, and dental anatomy. In any case, specimens of *O. microtis* and *Oligoryzomys* sp. n from eastern and central Amazon present slight differences in external characters, the most notable being the length of tail and coloration of dorsal, lateral and ventral parts. However, most characters show intra-populational variation.

The average HBL of the three populations groups are similar (Fig. 5A, table 2), but the tail length in specimens from the Eastern clade are significantly longer than in specimens from the Central clade and *O. microtis*, both in relative and absolute terms (Fig. 5B). The same is true for the length of the hindfeet (Fig. 5C), which also displays significative differences between the eastern group viz-a-viz central group and *O. microtis*

In terms of coloration (Fig. 6), most individuals from eastern populations have an orange-brown coloration (Villalobos-Dominguez and Villalobos 1947: color range from O-8-8º to 8-11-7º; Ridgway 1912: antique brown, buckhorn brown), with dark base of guard-hairs distinct and heterogeneous overall coloration, while individuals from central Amazon and *O. microtis* have a slightly lighter coloration (Villalobos-Dominguez and Villalobos 1947: color range from O-5-8º to 8-9-8º; Ridgway 1912: antique brown, brussels brown, raw umber). The ventral coloration of specimens from central Amazon and *O. microtis* vary from ochreous to white.

Oligoryzomys species are very similar cranially (Fig. 7), as most characters are either polymorphic within species or subtle variations of a general morphology, or both. In any case, the three lineages within *O. microtis* species group exhibit slight variation in a few characters that can be used for a differential diagnosis (Fig. 8 and sup. fig. 2).

Overall, members of the central populations are more dissimilar morphologically from Eastern clade and *O. microtis* specimens.

Most specimens (sup. fig. 2) from Amazonas and Acre states (*O. microtis*) and from Pará and Tocantins (Eastern clade) have a narrow zygomatic notch, oriented postero-laterally (Fig. 8A), with the anterior border of the zygomatic plate flat, below or slightly in front of anterior margin of superior maxillary root of zygoma; in contrast, most specimens from Rondônia and Mato Grosso (Central clade) have a slightly broad and rounded zygomatic notch (Fig. 8B), and a zygomatic plate with anterodorsal margin smoothly curved.

The interorbital region of all specimens of the Central clade are symmetrically constricted without crests (hourglass shape; fig. 8C), while in *O. microtis* and in the Eastern clade specimens can present either the amphoral morphology, or the interorbital region with margins slightly convergent anteriorly, with very weakly developed crests in their beaded supraorbital borders (cuneate shape; fig. 8D). The same pattern of variation is observed for the interparietal width: while the members of *O. microtis* and the Eastern clade have either narrower interparietal narrower, apart from the squamosal (Fig. 8E) or a wide interparietal approaching the squamosal (Fig. 8F), all members of the Central clade have a wide interparietal.

The jugal bone is present in the lateral surface of the zygomatic arch, separating the maxillary and squamosal bones (Fig. 8G), in few specimens from all analyzed populations (sup. fig. 2); in contrast, in most specimens the jugal is usually absent laterally (Fig. 8H), or extremely reduced to bony sliver, resulting in the maxillary and squamosal in contact.

The shape of the incisive foramina is also variable among the lineages (Fig. 8I-K). Most members of *O. microtis* and *Oligoryzomys* sp. n. from Eastern clade present

teardrop-shaped incisive foramina, with posterior margins rounded (Fig. 8I and K), while specimens from Central clade have oval-shaped foramina, with more pointed posterior margins (Fig. 8J). In terms of length, the foramina of specimens of all lineages of *O. microtis* are variable, not approaching the plane of M1 alveolus or barely approaching the line of M1 alveolus. Finally, the posterior extent of the palate is also slightly variable, with palate of intermediate length, mesopterygoid fossa extends up to 1/2 of M3 length between the maxillary bones (Fig. 8I), as observed in most specimens of Central clade and almost all from Eastern clade; or palate long, mesopterygoid fossa extend more than M3 length (Fig. 8J-K), as observed in more than half of specimens of *O. microtis*.

The descriptive statistics for cranial characters (Table 2) showed that members of the three geographic sets, *O. microtis* s.s., *Oligoryzomys* sp. n. from south-central Amazon, and *Oligoryzomys* sp. n from southeastern Amazon, are similar in size, with considerable overlap on mean and range sizes. Four cranial measurements displayed significant differences among the three population sets in the ANOVA: PB (p <0.001), BIF, LM, and ZB (p <0.05); nevertheless, only the first variable was significant after Holm-Bonferroni correction. The MANOVA recovered significant variation among the population sets (Wilks = 0.355, approx. F = 3.5, num. DF = 24, den. DF = 124, p = 2.575e-06). Pairwise Tukey tests showed that eastern populations of *Oligoryzomys* sp. n. to be significantly different (p <0.001) from central populations of *Oligoryzomys* sp. n. in two variables (PB and LM). *Oligoryzomys microtis s.s.* did not differ significantly in any variable from central or eastern population sets.

The three population sets of *O. microtis* species group were also poorly differentiated by principal component analysis (Fig. 9 and appendix 4). The scatterplots of the first two principal components, which account for 83% of the total variance, reveal an overall juxtaposition in the multivariate space (Fig. 9A). There is a large

amount of variation on the first component (77.21%), which is explained by variables associated to the cranial longitudinal axis, especially condylo-zygomatic length. Pairwise contrasts between the population sets (Fig. 9B-D) present the same pattern, with a slight separation between central and eastern forms of *Oligoryzomys sp. n.*, but with western *O. microtis* scores overlapping with central and eastern groups (*Oligoryzomys* sp. n.).

The discriminant canonical functions (Fig. 9E), in turn, reveal a significative separation among the three population sets (LR test = 0.577 approx. F = 3.8477, num. DF = 12, den. DF = 63, $p = 0.0002$), and is even more conspicuous when the contrasts are pairwise (Fig. 9F-H). Nevertheless, a considerable overlap among canonical function scores is observed in all contrasts.

Discussion

Karyotype variation

The karyotype of the central and eastern forms of *Oligoryzomys* sp. n., with 2n=64 and FN=64 is similar to the one of *O. microtis sensu stricto*, 2n=64 and FN=66 (Fig. 2, table 1). Although sharing the same diploid number, they differ in FN due to a pericentric inversion affecting the largest autosome pair of these karyotypes, being submetacentric in *O. microtis* and acrocentric in *Oligoryzomys* sp. n. (Fig. 2). This inversion is apparently fixed because heterozygous specimens for this inversion were neither found in the present study nor in previous reports (Gardner and Patton 1976, Aniskin and Volobouev 1999, Patton *et al*. 2000, Di-Nizo *et al*. 2015). The comparison of the G band karyotypes of *O. microtis* (2n=64 and FN=66, Aniskin and Volobouev 1999) and *Oligoryzomys* sp. n. (2n=64 and FN=64, Di-Nizo *et al*. 2015) allows us to infer homologies in large size pairs of the autosome complement, despite differences in the chromosome elongation. This

comparison corroborates that these karyotypes differ by one pericentric inversion or centromere shift affecting the largest autosome pair.

A considerable amount of evidence suggests deleterious meiotic effects of pericentric inversions leading to a profound barrier in viability, acting as a significant post-mating isolating mechanism (King 1993). Other examples of fixed pericentric inversion in congeneric sigmodontine species pairs are *Calomys tener* and *Calomys expulsus* (Bonvicino and Almeida 2000), *Cerradomys akroai* and *Cerradomys scotti* (Bonvicino *et al*. 2014), *Juliomys rimofrons* and *Juliomys ossitenuis* (Costa *et al*. 2007). Examples of pericentric inversion as polymorphism are in *Oligoryzomys nigripes* and *Akodon cursor* (Fagundes et al. 1998, Bonvicino et al. 2001).

The apparent similarity between the karyotype of *Oligoryzomys* sp. n. (2n=64 and FN=64) with those of *O. microtis* (2n=64 and FN=66), *O. mattogrossae* (2n=62 and FN=64), and *O. flavescens* (2n=64-66 and FN=66-68), has led to various incorrect associations (see Weksler and Bonvicino 2015). The karyotype of *Oligoryzomys* sp. n. with 2n=64 and FN=64 has been attributed to *O. microtis* (Di-Nizo *et al*. 2015). Another chromosome complement with 2n=66 and FN=74 (Andrades-Miranda *et al.* 2001) was described from Amazonian *Oligoryzomys* specimens wrongly identified as *O. microtis*; this karyotype probably belongs to *O. messorius* (see Weksler and Bonvicino 2015).

The chromosome complements of *O. microtis* (2n=64 and FN=66) and *O. flavescens* (2n=64 and FN=66), despite sharing the same 2n and FN, differ in the morphology of the largest autosome pair, which is metacentric in the *O. microtis* and acrocentric in *O. flavescens,* despite sharing the same G banding pattern (Figure 3 in Aniskin and Volobouev 1999). The comparison of the complete G band karyotypes of *O. microtis* and *O. flavescens* shows variations in the morphology of the two largest autosome pairs. These differences arise from a centromeric shift and the addition of a heterochromatic

arm, respectively, indicating that these chromosomal features are stable within each species (Aniskin and Volobouev 1999). These karyotypes also differ from each other by the presence of supernumerary chromosomes in *O. flavescens*. Similarly, despite the apparent similarity between *O. mattogrossae* and *Oligoryzomys* sp. n. karyotypes, in situ hybridization clearly shows differences between the chromosome complements (Di-Nizo *et al*. 2015, species identified as *O. fornesi* and *O. microtis*, respectively). These findings also showed that these apparent similarities among *O. microtis*, *Oligoryzomys* sp. n., *O. mattogrossae*, and *O. flavescens* are superficial, and that the differences among these karyotypes are enough to reduce or prevent the fertility of hybrids.

Phylogenetic results

The phylogenetic analyses in this study, employing both Maximum Likelihood (ML) and Bayesian Analysis (BA) methods based on the mitochondrial cytochrome b gene (mt-Cytb) and the combined mt-Cytb and nuclear i7-Fgb, produced incongruent topologies, but the discrepancies were usually in clades with low support values. In the mt-Cytb-only analysis, the first split within *Oligoryzomys* separates the *O. microtis* species group from remaining species, while the combined analysis of mt-Cytb and the i7-Fgb gene reveals an initial dichotomy separating a clade with the *O. microtis* species group and *O. mattogrossae* from the remaining species. Four additional clades are strongly supported in both mt-Cytb and the combined analyses: 1) *O. stramineus* + *O. nigripes*, 2) *O. occidentalis* + *O. longicaudatus* + *O. flavescens* + *O. fornesi*, 3) *O. costaricensis* + *O. vegetus* + *O. fulvescens, O. destructor*, and 4) *O. arenalis* + *O. guille, O. andinus*. These findings provide insights into the phylogenetic relationships and genetic divergence within the *Oligoryzomys* genus, aligning with previous phylogenetic analyses of the

genus (e.g., González-Ittig et al. 2010, 2014, Weksler et al. 2017, da Cruz and Weksler 2018, da Cruz et al. 2019, Hurtado and D'Elía 2019, 2022).

The *O. microtis* species group, as identified in this study, comprises two primary clades. The first clade encompasses *O. microtis sensu stricto* specimens from Peru, Bolivia, and the Brazilian states of Acre and Amazonas within the western Amazon, including the topotype specimen MN84349. The second clade comprises specimens of *Oligoryzomys* sp. n. from Tocantins, Mato Grosso, and Rondônia. Significantly, this clade is further divided into two well-supported subclades, each characterized by distinct geographic distributions. The first subclade, referred to as the Central clade, includes samples from Mato Grosso and Rondônia, located in the south-central Amazon region, while the second subclade, known as the Eastern clade, encompasses specimens from Tocantins, positioned in the southeastern Amazon region.

Additionally, the median-joining network analysis of mt-Cytb data delineates three primary haplogroups. The first corresponds to *O. microtis* s.s., with specimens from Bolivia, Peru, and the Brazilian states of Amazonas and Acre. The second comprises specimens of *Oligoryzomys* sp. n. from the Brazilian state of Rondônia (Central clade), and the third includes specimens from Tocantins (Eastern clade). Within the first haplogroup, there is further subdivision into two subgroups. One subgroup contains specimens from Peru and the Brazilian states of Amazonas and Acre, while the other comprises specimens from Bolivia and the Brazilian state of Acre. Genetic distances, based on uncorrected p-distances using mt-Cytb sequences, reveal a 7.4% difference between *O. microtis* s.s. and *Oligoryzomys* sp. n. Eastern clade, a 7.4% difference between *O. microtis* s.s. and *Oligoryzomys* sp. n. Central clade, and a 5.4% difference between the central and Eastern clades of *Oligoryzomys* sp. n. This intricate genetic structuring within the *O. microtis* species group alludes to potential historical isolation

and differentiation events within these regions, underscoring the genetic distinctiveness of *Oligoryzomys microtis* from the western Amazon, including those from the type locality, in comparison to their counterparts in the south central and southeastern Amazon regions.

Morphological variation and cryptic species

Species of the genus *Oligoryzomys*, and in particular Amazonian forms, are extremely similar in their external and cranial anatomy, and thus very hard to tell apart; Hershkovitz (1966: 137), for instance, considered *O. flavescens* and *O. longicaudatus* as "races" of *O. nigripes*. Moreover, Voss et al. (2001: 119) stated that they "…found no obvious qualitative characters to distinguish *Oligoryzomys fulvescens* (as represented by … Mexican and central American exemplars) from typical *O. microtis*." Despite overall similarity, several morphological characters have been demonstrated to vary among species (Myers and Carleton 1981, Carleton and Musser 1995, Weksler and Bonvicino 2005, Machado et al. 2011, Agrellos et al. 2012, Weksler et al. 2017, Hurtado 2021), and a few subtle differences were observed among the mitochondrial lineages detected here, such as configuration of interorbital region, incisive foramina, zygomatic plate, and jugal. In any case, *O. microtis* and *Oligoryzomys* sp. n. are so morphologically and morphometrically similar that they can be considered as cryptic species, at least in the character systems analyzed by us. Additional research in comparative morphology of other character systems, such as penial and stomach morphology, may reveal diagnostic characteristics for the species.

Numerous other *Oligoryzomys* species present taxonomic challenges as cryptic entities. These species exhibit limited and often polymorphic morphological variations while concurrently demonstrating significant divergence in karyological and molecular

characteristics (González-Ittig et al. 2014, Rivera et al. 2018, da Cruz and Weksler 2018). The complexities surrounding their identification hold substantial implications, particularly in the context of public health services, as several *Oligoryzomys* species serve as reservoirs for *Orthohantavirus* (Agrellos et al. 2012, Firth et al. 2012, Rivera et al. 2007, da Cruz et al. 2019).

Within rodents, and more broadly among mammals, the discovery of cryptic species currently lies on the application of molecular techniques, with "DNA barcoding" and automatic species detection (e.g., GMYC, b-PTP) standing as popular tools for unraveling genetic variations within seemingly indistinguishable populations (e.g., da Cruz et al. 2019, Ojeda et al. 2021, Di-Nizo et al. 2022, Quiroga-Carmona et al. 2022). Nevertheless, the central challenge in recognizing cryptic species lies in distinguishing between genetic structuring arising from geographical barriers within a species and the delineation of genuinely distinct evolutionary lineages that may exhibit morphological similarities. We contend that karyotypic data serves as an indispensable source of information for distinguishing between genuine cryptic entities and regional variants marked by genetic structuring. This rationale underpins the approach adopted in our current study, where we describe a new species possessing a distinctive karyotype in contrast to *O. microtis*, while the two new subspecies share the same karyotype and exhibit subtle morphological differences. We further emphasize the need for expanded and more geographically comprehensive sampling to validate our classification.

Biogeography

Oligoryzomys sp. n. predominantly inhabits the central Brazil Shield, while *O. microtis sensu stricto* is found in the western Amazonia lowlands and in the Mamoré-Madre de Dios Piedmont. The new lineage is currently separated from *O. microtis* in the

northern part of its range by the Amazonas/Solimões River, and in the west by its tributary, the Madeira River. This distribution pattern is also observed in marsupials, as seen with *Monodelphis glirina* with distribution in the western Amazonia lowlands and its sister species, *M. maraxina*, in the central Brazil Shield (Bonvicino et al. 2023). The Amazonas/Solimões River also serves as a barrier for subspecies and sister species of various mammals, including rodents such as *P. steerei* in the south and *P. quadruplicatus* in the north (Patton and Siva 1998). Additionally, marsupials such as *Caluromys philander philander* are found in the north, while *C. philander affinis* and *C. philander dichurus* inhabit the south. In the case of species of *Marmosa (Micoureus), M. demerarae* is found in the north of the Amazonas/Solimões River, while *M. constantiae* and *M. domina* are located in the south (Bonvicino et al. 2023).

There is evidence that the Madeira River has acted as a vicariance barrier for certain mammals and avian species, such as Primates like *Callicebus brunneus* and *Callicebus dub*ius (Santorelli et al. 2018), as well as birds like *Psophia viridis* and *Psophia leucoptera* (Ribas et al. 2011). However, its role as the limit of distribution was not supported for several species of mammals, birds and squamates (Santorelli et al. 2018).

The hypothesis of rivers serving as current barriers has been tested since its formulation in the 19th century (Wallace 1853) and has become a valuable concept for understanding the delimitation of species and subspecies distribution. Riverine barriers can pose significant obstacles to several taxa, such as birds (Naka et al. 2022) and mammals (Ayres and Clutton-Brock 1992). However, the role of rivers as a primary factor in speciation remains less established (Bonvicino and Weksler 2012, Janiak et al. 2022). When assessing the role of rivers as geographic barriers, it is essential to consider various characteristics, not only of the rivers themselves (e.g., meandering rivers, depth, water speed) but also of the taxa under investigation, including their ability to disperse

and swim. In the case of *Oligoryzomys* sp. n., the causative role of the Madeira River remains uncertain.

O. microtis *taxonomy and implications for Rio Mamoré orthohantavirus*

Karyotype differences were congruent with median-joining and phylogenetic analyses (Figs. 3 and 4), which showed *O. microtis* separated into two clades, the first with specimens from Brazilian Cerrado biome and transitions areas with Amazonas, including karyotyped animals of *Oligoryzomys* sp. n.; and a second clade with specimens from localities in the Bolivian, Peruvian and Brazilian Amazon biome, including karyotyped specimens, and a topotype, of *O. microtis*. The first clade was further divided into two subclades, one with specimens from southeastern Amazon (Tocantins state) and another with specimens from south central Amazon (Rondônia and Mato Grosso states).

Previous studies with *Orthohantavirus* sequences detected four variants in the Rio Mamoré orthohantavirus genotype (Richter et al. 2010, Firth et al. 2012, Guterres et al. 2015, Nunes et al. 2015): RIOMV in Bolivia (=OMM-556) and in Peru (=HTN-007), RIOMV-3 in Acre and Amazonas states, Brazil; and RIOMV-4 in Rondônia state, Brazil. Phylogenetic analysis of *Orthohantavirus* sequences (Firth et al. 2012) have demonstrated that these four lineages are highly divergent and do not form monophyletic groups. These authors also associated the first three lineages of Rio Mamore orthohantavirus to *O. microtis* and one, RIOMV-4, to an unnamed species, which is described here (see also Figure 3 for identification of *Orthohantavirus* positive *Oligoryzomys* specimens).

The evidence presented here suggests that *O. microtis* and *Oligoryzomys* sp. n. belong to different evolutionary lineages, and thus they merit taxonomic recognition. Although the two forms are reciprocally monophyletic and differ in the chromosomal complement,

they are morphologically similar, and thus could be considered as different cryptic species in a phylogenetic species concept (e.g., de Queiroz 2007). Furthermore, we opted here for the recognition of two subspecies within the *Oligoryzomys* sp. n. lineage, corresponding to the Central and Eastern clades, due to sharing the same karyotype. We could not find non-overlapping discrete morphological diagnostic features between the two subspecies among analyzed features (skin, skull, and dentition), and thus taxonomic identification would be presently impossible without the use of DNA sequences, hindering ecological and epidemiological studies. Future morphological work in other anatomical systems may provide anatomical evidence for specific separation.

TAXONOMIC ACCOUNT

***Oligoryzomys gri* sp. n.**

Figures 6, 7, and 8

Zoobank registration. This nomenclatural act is registered in ZooBank: urn:lsid:zoobank.org:pub:AB82ECCE-1969-4A2F-AFFD-7FA5B17A784E

Holotype. MN87921, an adult male collected on 2005, July 20 by Secretaria de Vigilância em Saúde (SVS, original field number SVS134/LBCE20531), at Fazenda do Seu Bento, Alto Paraíso, Rondônia state, Brazil (Fig. 7). The holotype consists of skin, skull, and liver tissue fixed in ethanol. External measurements of holotype (see material and methods for acronyms; all measurements in mm except weight): ToL = 185, TL = 101, HF = 20, Ear = 13, W = 13 g, CIL = 21.01, LD = 5.74, PB = 4.45, LIF = 3.57, BIF = 1.62, LM = 3.40, BM1 = 1.01, M1M = 4.25, BRO = 4.35, ORL = 8.05, ZB = 12.19, BZP = 2.17.

Paratypes. All from the type locality. MN91084, an adult male (original field number SVS003/LBCE7038), and MN91085, an adult female (original field number

SVS004/LBCE7039), both collected by SVS on 2005, July 15, consisting of skin, skull (broken), cell suspension and liver tissue fixed in ethanol. MN87919 male (original field number SVS118/LBCE20515), collected by SVS on 2005, July 20, consisting of skin, skull, and liver tissue fixed in ethanol; MN91086 male (original field number SVS107), collected by SVS on 2005, July 19, consisting of skin, skull (broken), and liver tissue fixed in ethanol.

Etymology: the name *gri* means small or tiny in the Apinayé language (Albuquerque 2012), as well as in proto-Macro-Jê (Nikulin 2020), and refers to the smaller size of this species in relation to most *Oligoryzomys* species. We employed the Latin form 'gri', as employed in Albuquerque (2012), instead of 'ŋgri' (Nikulin 2020) because the guttural sound represented by the letter 'ŋ' can be challenging to pronounce.

Type Locality: Brazil, Rondônia state, Alto Paraíso, Fazenda do Seu Bento (9º19'15"S, 63º19'15"W, 108 m a.s.l.).

Geographic Distribution: *Oligoryzomys gri* sp. n. occurs throughout the Southern border of the Amazon biome of central and northwest Brazil and in areas of ecotone between Amazon and Cerrado biomes (Fig. 1; appendix 1). In Brazil, the species has been reported in the states of Rondônia, Mato Grosso, Pará, and Tocantins (Table 1, fig. 1), in the Madeira-Tapajos and Xingu-Tocantins interfluvial regions.

Diagnosis: A small-sized *Oligoryzomys* species (adult HBL varying from 73-105 mm) with slightly bicolored tail longer than the head-body size, incisive foramina posterior borders never extending posteriorly the plane of the alveolus of the first upper molars, palatal bridge broad and relatively short, with posterior portion extending beyond M3 plane less than half M3 length. In addition, all known karyotyped specimens share the same diploid number of 64 and fundamental autosome number of 64.

Description: Adult dorsal pelage yellowish to orangish brown (brussels brown, raw umber, antique brown, buckhorn brown in Ridgway 1912), composed of ca. 6-7 mm-long guard hairs and slightly shorter overhairs with a sub-apical brown-yellowish or brown-orangish band (Fig. 6). Lateral color lighter than in dorsum and with a defined limit with the ventral pelage. Ventral pelage coloration varies from light cream to white slightly tinged with ochre; younger animals have more ochraceous overtones. Ventral hairs are cream at their upper part and grey in the third or fifth basal part. Gular and urogenital region with pure cream hairs, without any basal grey band. Dorsal surface of pes with short pelage, with cream hairs. Short tufts of white ungual hairs at bases of claws on dII–dV. Plantar surface of pes with conspicuous scales and with six plantar pads. Internal hairs of the ear are light brown. Tail longer than combined length of head and body, scarcely covered with small brown light hairs, and covered with relatively conspicuous epidermal scales, lacking a long tuft of terminal hairs and weakly bicolored, dorsal surface dark grey and ventral surface light grey. Superciliary, genal, and mystacial vibrissae do not extend beyond ears. See table 2 for external measurements.

Delicate skull (Figs. 7 and 8), narrow rostrum, but slightly wider than interorbital constriction. Interorbital region hourglass-shaped or very slightly cuneate in eastern populations. Braincase without supraorbital (or weakly developed in eastern populations) and postorbital ridges. Interparietal bone as broad as anterior half of parietal. Relatively large zygomatic plate with shallow or moderate zygomatic notch. Jugal bone not detected in lateral view, resulting in zygomatic process of squamosal in contact with the zygomatic process of maxillary. Incisive foramina teardrop or round bracket shaped, the posterior borders not reaching or reaching (in eastern populations) the plane of the alveolus of the first upper molars, but never extending posteriorly. Palatal bridge broad and relatively short, with posterior portion extending beyond M3 plane, less than half M3 length. Palate

with one single large, or two smaller, posterolateral palatal pits recessed, or not, in an incipient palatine fossa situated anterior to mesopterygoid fossa and posterior or lateral to M3. Bony roof of mesopterygoid fossa perforated by large sphenopalatine vacuities. Width of parapterygoid plate similar to the width of mesopterygoid fossa. Alisphenoid strut absent (buccinator-masticatory foramen and accessory foramen ovale confluent), alisphenoid canal with large anterior opening. Stapedial foramen and the posterior opening of the alisphenoid canal large, but squamosal–alisphenoid groove and sphenofrontal foramen absent (= carotid circulatory pattern 2 of Voss 1988). Posterior suspensory process of the squamosal absent. Large subsquamosal fenestra, slightly smaller than postglenoid foramen. Periotic exposed posteromedially between ectotympanic and basioccipital, reaching the carotid canal. Mastoid perforated by conspicuous postero-dorsal fenestra. In mandible, capsular process of lower incisor alveolus well developed; superior and inferior masseteric ridges converging anteriorly as open chevron below m1.

Upper and lower incisors opisthodont; molars pentalophodont. Superior molar rows parallel. Procingulum of first upper molar (M1) with anteromedian flexus only in young animals, with moderate wear lacking anteromediam flexus. A small anteroloph is present and separate from anterocone in young, but anteroloph is joined with anterocone in specimens with more advanced wear; posteroloph small joined to metacone in specimens with more advanced wear. Paracone connected to mesoloph, creating an internal mesofosseta. M2 with mesoloph, with or without a protoflexus. Third upper molar (M3) is reduced, and has a single posterior cusp, which we equate to the hypocone; hypoflexus is diminutive. The anteroconid of the first lower molar (m1) is without an anteromedian flexid; the mesolophid is distinct on unworn m1 and m2; m2 and m3 with anterolabial cingulum.

Karyotype: This species is characterized by 2n=64 and FN=64. Because of the poorly known taxonomy of this group of species, this karyotype has been previously associated with *O. microti*s (Di-Nizo *et al*. 2015), and *O. flavescens* (Lima 2004, Table 1).

Habitat: *Oligoryzomys gri* sp. n. is an inhabitant of Cerrado and transition areas with Amazonas.

Comparisons: *Oligoryzomys* species are very similar one to another, and few characters allow the separation between them**.** *Oligoryzomys gri* sp. n. differs from all other *Oligoryzomys* species by its unique karyotype. In addition, *O. gri* sp. n. differs from *Oligoryzomys* species that occur in Brazil by a combination of other characters including (1) slightly bicolored tail, contrary to unicolored tail in *O. nigripes* and *O. rupestris* (other species of the genus also have slightly bicolored tails); (2) small-sized species (adult HBL between < 87 mm in average) as in *O. rupestris*, *O. microtis*, *O. moojeni*, *O. flavescens*, *O. delicatus*, *O. messorius*, *O. fornesi*, *O. mattogrossae*, opposed to large size species (adult HBL > 100 mm in average) as *O. nigripes*, *O. stramineus*, and *O. chacoensis*. *O. gri* sp. n. is different from *O. microtis* in the relatively smaller incisive foramen in relation to the diastema length. See also results above for more detailed morphological contrasts with *O. microtis.*

Conservation status: *Oligoryzomys gri* sp. n. inhabits the region of the ecotone between the Amazon rainforest and Cerrado of Central and Northern Brazil, currently undergoing massive development in the "agricultural frontier", where cases of Hantavirus pulmonary syndrome (HPS) have been reported (Oliveira et al. 2009, Oliveira et al. 2011, Rosa et al., 2005, Rosa et al., 2010, Suzuki et al., 2004). This new species, as far as we know, is not uncommon at its sampling sites, with several specimens collected during field work. Despite its extensive geographic range (Fig. 1), sampling localities were relatively few

and distant among them. We propose that the species be categorized as data-deficient until further information is acquired for a proper evaluation by IUCN criteria.

Remarks: Hurtado and D´Elía (2019) suggested the presence of two new candidate species within the *O. microtis* complex in their analysis of molecular variation and automatic species identification; the two candidate species would represent the Central and Eastern clades detected in our phylogenetic analyses and considered here as subspecies of *Oligoryzomys gri* sp. n.: *O. gri gri,* and *O. gri apinaye*, described below, respectively.

Specimens Examined: See appendix 1.

***Oligoryzomys gri apinaye* subsp. n.**

Figures 6, 7 and 8

Zoobank registration. This nomenclatural act is registered in ZooBank: urn:lsid:zoobank.org:act:1ABF99F0-2792-4B72-BD87-A2EFDF172281

Holotype: MN76206 an adult male, collected on September 1997 by Laboratório de Vertebrados, UFRJ (original field number FO19), at Fazenda Osara II, São Sebastião do Tocantins, Tocantins state, Brazil (Fig. 7). The holotype consists of skin, skull, and liver tissue fixed in ethanol. External measurements of holotype (see material and methods for acronyms; all measurements in mm except weight): ToL = 193, TL = 103, HF = 23, Ear = 14, W = 23 g, CIL = 21.52, LD = 5.77, PB = 3.89, LIF = 4.28, BIF = 1.79, LM = 3.37, BM1 = 0.95, M1M = 4.23, BRO = 4.35, ORL = 7.98, ZB = 12.64, BZP = 2.29.

Paratypes: All from type locality consisting of skin, skull, and tissues. MN76192 (original field number FO05), MN76194 (FO07), MN76198 (FO10), MN76200 (FO13), MN76203 (FO16), MN75205 (FO18), MN76207 (FO20), MN76209 (FO22), MN76210

(FO23), MN76212 (FO25), MN76213 (FO26), MN76216 (FO29), MN76217 (FO30), MN76223 (FO36), MN81726 (FO41), MN76226 (FO43), MN81727 (FO44), MN76227 (FO45), MN80436 (FO47), MN80431 (FO39). Skin, skull, tissue and cells suspension of MN81639 (offspring of MN81726), MN81640 (offspring of MN81726), MN81641 (offspring of MN81727), MN81642 (offspring of MN81727), MN81643 (offspring of MN81726), and MN81644 (offspring of MN81726).

Etymology: The name refers to the Apinayé people of the Macro-Jê linguistic trunk, who are the native inhabitants of the north of the State of Tocantins, mainly around the rivers Araguaia and Tocantins.

Type locality: Brazil, Tocantins state, São Sebastião do Tocantins municipality, Fazenda Osara II (5º16'S, 48º21'W).

Geographic distribution: *Oligoryzomys gri apinaye* ssp. n. occurs in south-eastern Amazon, in the moist and semi-deciduous forests of the Xingu-Tocantins/Araguaia interfluvial region and in areas of ecotone between Amazon and Cerrado biomes, in the Brazilian states of Tocantins and Pará (Fig. 1).

Diagnosis: A small-sized *Oligoryzomys* taxon (adult HBL varying from 78-99 mm) with tail longer than the head-body size, and characterized by the combination of the following morphological characteristics: interorbital region cuneate with weakly developed supraorbital ridges; large zygomatic plate with deep zygomatic notch; palatal bridge broad and long, with posterior portion extending beyond M3 plane by half M3 length.

Description: External morphology as in *Oligoryzomys gri* (Fig. 6), except for characters differentiated in the diagnosis (see also fig. 5). See table 2 for external measurements. Skull similar to *O. gri*, except in the following characters (Fig. 7 and 8): interorbital region cuneate; supraorbital ridges weakly developed. Relatively large zygomatic plate with deep zygomatic notch. Incisive foramina reaching the plane of the alveolus of the first

upper molars, but never extending posteriorly. Palatal bridge broad and long, with posterior portion extending beyond M3 plane by half M3 length. Long mesopterygoid fossa exposing a relatively larger portion of the presphenoid.

Karyotype: This species is characterized by 2n=64 and FN=64 (Fig. 2), sharing the same chromosome complement with *Oligoryzomys gri gri*.

Habitat: *Oligoryzomys gri apinaye* subsp. n. is an inhabitant of Cerrado and transition areas with the Amazon.

Comparisons: See comparisons above for contrasts with other species**.** *Oligoryzomys gri apinaye* ssp. n. differs from *Oligoryzomys gri gri* by its smaller skull size (Table 2), deeper zygomatic notch and longer interparietal and the cuneate supraparietal region with more developed crests (Figs. 7 and 8). In ventral view, *O. gri apinaye* differs from both *O. gri gri* and *O. microtis* in longer incisive foramen, resulting in a shorter palatal bridge, and a mesopterygoid fossa extending anteriorly closer to M3 plane (less than M3 length; fig. 8).

Remarks: See above in remarks for *Oligoryzomys gri* sp. n..

Specimens Examined: This subspecies corresponds to *Oligoryzomys* sp. in Hurtado and D´Elía (2019) and to clade 2 of *O. microtis* in da Cruz et al. (2019).

Acknowledgments

We appreciated the collaboration in fieldwork by the field team of Secretaria de Vigilância em Saúde (SVS), Laboratório de Biologia e Parasitologia de Mamíferos Silvestres Reservatórios, IOC, FIOCRUZ, and Laboratório de Vertebrados (UFRJ). Instituto Chico Mendes de Conservação da Natureza (ICMBio) granted license to collect the specimens. Work was supported by grants from the Conselho Nacional de Desenvolvimento Científico e Tecnológico (CNPq) to M. Weksler (440663/2015-6 and 309654/2020-3) and C. R. Bonvicino (304498/2014-9 and 312446/2018-7), and from the Fundação de Amparo à Pesquisa do Estado do Rio de Janeiro (FAPERJ) to M. Weksler (E-26/110.505/2012 and E-26/201.232/2022) and C. R. Bonvicino (E26/201.200/2014 and E-26/210.047/2014). We also would like to thank the curators and staff from the AMNH (Robert S. Voss, Nancy Simmons, and Eileen Westwig), USNM (Alfred Gardner, Michael Carleton), and MN/UFRJ (João A. de Oliveira). We are grateful to one anonymous reviewer and P. Gaubert for fruitful comments on the original draft.

References

Agrellos R., Bonvicino C.R., Rosa E.S.T., Marques A.A.R., D'Andrea P.S., Weksler M., 2012. The taxonomic status of the Castelo dos Sonhos Hantavirus reservoir, *Oligoryzomys utiaritensis* Allen 1916 (Rodentia, Cricetidae, Sigmodontinae). Zootaxa 3220: 1–28.

Albuquerque F.E., 2012. Dicionário escolar Apinayé. Editora da Faculdade de Letras da Universidade Federal de Minas Gerais, Belo Horizonte, Brazil.

Almendra A.L., Rogers D.S., González-Cózatl F.X., 2014. Molecular phylogenetics of the *Handleyomys chapmani* complex in Mesoamerica. J. Mammal. 95**:** 26–40.

Andrades-Miranda J., Oliveira L.F.B., Lima-Rosa C.A.V., Nunes A.P., Zanchin N.I.T., Mattevi M.S., 2001. Chromosome studies of seven species of *Oligoryzomys* (Rodentia, Sigmodontinae) from Brazil. J. Mammal. 82(4): 1080–1091. doi:10.1644/1545-1542(2001)082<1080:CSOSSO>2.0.CO;2

Aniskin V.M., Volobouev V.T., 1999. Comparative chromosome banding of two South-American species of rice rats of the genus *Oligoryzomys* (Rodentia, Sigmodontinae). Chromosome Res. 7: 557–562. doi:10.1023/a:1009245729902

Ayres J. M., Clutton-Brock T. H., 1992. River boundaries and species range size in Amazonian Primates. Amer. Natural. 140(3): 531 –537.

Bandelt H.J., Forster P., Röhl A., 1999. Median-joining networks for inferring intraspecific phylogenies. Mol. Biol. Evol. 16(1): 37–48.

Bharadwaj M., Botten J., Torrez-Martinez N., Hjelle B., 1997. Rio Mamore virus: genetic characterization of a newly recognized hantavirus of the pygmy rice rat, *Oligoryzomys microtis*, from Bolivia. Am. J. Trop. Med. Hyg. 57:368–374. doi:10.4269/ajtmh.1997.57.368.

Bonvicino C.R., Almeida F.C., 2000. Karyotype, morphology and taxonomic status of *Calomys expulsus* (Rodentia: Sigmodontinae). Mammalia 64(3): 339–351. doi:10.1515/mamm.2000.64.3.339.

Bonvicino C.R., Moreira M.A., 2001. Molecular phylogeny of the genus *Oryzomys* (Rodentia: Sigmodontinae) based on cytochrome b DNA sequences. Mol. Phylogen. Evol. 18: 282–92.

Bonvicino C.R., Weksler M., 1998. A new species of *Oligoryzomys* (Rodentia, Sigmodontinae) from northeastern and central Brazil. Z. Saügetierk. 63: 90–103.

Bonvicino C.R., Weksler M., 2012. Speciation in Amazonia: Patterns and Predictions of a Network of Hypotheses. In: Patterson B.D., Costa E.P. (Eds.) Bones Clones and Biomes. University of Chicago Press, Chicago, Il. 283-306.

Bonvicino C.R., Casado F., Weksler M., 2014. A new species of *Cerradomys* (Mammalia: Rodentia: Cricetidae) from central Brazil, with remarks on the taxonomy of the genus. Zoologia (Curitiba) 31(6): 525–540. doi:10.1590/S1984-46702014000600002

Bonvicino C.R., D'Andrea P.S., Borodin P., 2001. Pericentric inversions: a study in natural populations of *Oligoryzomys nigripes* (Rodentia: Sigmodontinae). Genome 44: 791–796. doi:10.1139/g01-080.

Bonvicino C.R., Lazar A., Freitas T., Lanes R.O., D'Andrea PS, 2023. Diversification of the Marsupials (Didelphimorphia) of South America. In: Cáceres N.C., Dickman C. R. (Eds.) American and Australasian Marsupials. An Evolutionary, Biogeographical, and Ecological Approach. Springer Nature, Cham, Switzerland.

Bordignon S.E., 2007. Análise da variabilidade cromossômica e distribuição geográfica de duas espécies de *Oligoryzomys* (Rodentia, Cricetidae) ocorrentes nos Estados de Santa Catarina e Paraná. Honors Thesis, Universidade Federal do Paraná, Curitiba, Brazil.

Brum-Zorilla N., Fronza T.G., Wainberg R., Vidal-Rioja I., Zwinrger N., 1988. *Oryzomys flavescens* and *O delticola* chromosomes (Rodentia, Cricetidae) from Uruguay and Argentina. Caryologia 41: 275–288. doi:10.1080/00087114.1988.10797868

Canon C., Mir D., Pardiñas U.F.J., Lessa E.P., D'Elía G., 2014. A multilocus perspective on the phylogenetic relationships and diversification of rodents of the tribe Abrotrichini (Cricetidae: Sigmodontinae). Zool. Scr. 43**:** 443–454.

Carleton M.D., Musser G.G., 1989. Systematic studies of oryzomyine rodents (Muridae, Sigmodontinae): a synopsis of *Microryzomys*. Bull. Am. Mus. Nat. Hist. 191: 1–83.

Carleton, M.D., Musser, G.G. 1995. Systematic studies of oryzomyine rodents (Muridae: Sigmodontinae): definition and distribution of *Oligoryzomys vegetus* (Bangs, 1902). Proc. Biol. Soc. Wash. 108(2): 338–369.

Carroll D.S., Mills J.N., Montgomery J.M, Bausch D.G., Blair P.J., Burans J.P., Felices V, Gianella A., Iihoshi N., Nichol S.T., Olson J.G., Rogers D.S., Salazar M., Ksiazek T.G., 2005. Hantavirus pulmonary syndrome in central Bolivia: relationships between reservoir hosts, habitats, and viral genotypes. Am. J. Trop. Med. Hyg. 72: 42–46.

Casado F., Bonvicino C.R., Nagle C., Comas B., Manzur T.D., Lahoz M.M., Seuánez H.N., 2010. Mitochondrial divergence between 2 populations of the hooded capuchin, *Cebus* (*Sapajus*) *cay* (Platyrrhini, Primates). J. Hered. 101: 261–269.

Casapía M., Mamani E., García M.P., Miraval M.L., Valencia P., Quino A.H., Donaires L.F., 2012. Síndrome pulmonar por Hantavirus (Virus Río Mamoré) en la Amazonía Peruana. Rev. Peru. Med. Exp. Salud. Pub. 29:390–395. doi:10.1590/s1726-46342012000300016

Castillo Oré R.M., Forshey B.M., Huaman A., Villaran M.V., Long K.C., Kochel T.J., Guevara C., Montgomery J.M., Alvarez C.A., Vilcarromero S., Morrison A.C., Halsey E.S., 2012. Serologic Evidence for Human Hantavirus Infection in Peru. Vector-Borne Zoonotic Dis. 12(8) :683–689. doi:10.1089/vbz.2011.0820

Costa L.P., Pavan S.E., Leite Y.L.R., Fagundes V., 2007. A new species of *Juliomys* (Mammalia: Rodentia: Cricetidae) from the Atlantic Forest of southeastern Brazil. Zootaxa 1463: 21–37.

da Cruz M.O.R., Weksler M., Bonvicino C.R., Bezerra A.M.R., Prosdocimi F., Furtado C., Geise L, Catzeflis F., Thoisy B. de, Oliveira L.F.B. de, Silva C., Oliveira J.A.

2019. DNA barcoding of the rodent genus *Oligoryzomys* (Cricetidae: Sigmodontinae): mitogenomic-anchored database and identification of nuclear mitochondrial translocations (Numts). Mitochondrial DNA Part A 17:1–11. Do:0.1080/24701394.2019.1622692

da Cruz M.O.R., Weksler M., 2018. Impact of tree priors in species delimitation and phylogenetics of the genus *Oligoryzomys* (Rodentia: Cricetidae). Mol. Phylogenet. Evol. 119: 1–12. doi:10.1016/j.ympev.2017.10.021.

de Andrade A.F.B., Bonvicino C.R., 2003. A new karyologic variant of *Oecomys* (Rodentia: Sigmodontinae) and its phylogenetic relationship based on molecular data. Genome 46(2): 195–203. doi:10.1139/g02-123

D'Elía G., Hanson J.D., Mauldin M.R., Teta T., Pardiñas U.F.J., 2015. Molecular systematics of South American marsh rats of the genus *Holochilus* (Muroidea, Cricetidae, Sigmodontinae). J. Mammal. 96 (5): 1081–1094. doi:10.1093/jmammal/gyv115.

De Queiroz K. 2007. Species Concepts and Species Delimitation. Syst. Biol. 56(6): 879–886. doi:10.1080/10635150701701083.

Di-Nizo C.B., Ventura K., Ferguson-Smith M.A., O'Brien P.C.M., Yonenaga-Yassuda Y., Silva M.J., 2015. Comparative Chromosome Painting in Six Species of *Oligoryzomys* (Rodentia, Sigmodontinae) and the Karyotype Evolution of the Genus. PLoS ONE 10(2): e0117579. doi:10.1371/journal. pone.0117579

Di-Nizo C.B., Suárez-Villota E.Y., Silva M.J.J., 2022. Species limits and recent diversification of *Cerradomys* (Sigmodontinae: Oryzomyini) during the Pleistocene. PeerJ 10: e13011. doi:10.7717/peerj.13011.

Drummond A. J., Rambaut A. 2007. BEAST: Bayesian evolutionary analysis by sampling trees. BMC Evolutionary Biology 7(1): 214.

Eppig J.T., Blake J.A., Bult C.J., Kadin J.A., Richardson J.E., The Mouse Genome Database Group. 2015. The Mouse Genome Database (MGD): facilitating mouse as a model for human biology and disease. Nucleic Acids Res. 28: D726–36.

Espinosa M.B., Reig O.A., 1991. Cytogenetics and karyosystematics of South American oryzomyine rodents (Cricetidae, Sigmodontinae) III. Banding karyotypes of Argentinian *Oligoryzomys*. Z. Säugetierk. 56: 306–317.

Fagundes V., Christoff A.U., Yonenaga-Yassuda, Y., 1998. Extraordinary chromosomal polymorphism with 28 different karyotypes in the neotropical species Akodon cursor (Muridae, Sigmodontinae), one of the smallest diploid number in rodents (2n=16, 15 and 14). Hereditas 129: 263–274. doi:10.1111/j.1601-5223.1998.00263.x

Felsenstein J., 1981. Evolutionary trees from DNA sequences: a maximum likelihood approach. J. Mol. Evol. 17: 368–76.

Felsenstein J., 1985. Confidence limits on phylogenies: an approach using the bootstrap. Evol. 39: 783–791.

Firth C., Tokarz R., Simith D.B., Nunes M.R.T., Bhat M., Rosa E.S.T., Medeiros D.B., Palacios G., Vasconcelos P.F.C., Lipkin W.I., 2012. Diversity and distribution of hantaviruses in South America. J. Virol. 86: 13756–66.

Friendly M., and Fox J., 2010. Candisc: R package for canonical discriminant analysis.

Gardner A.L., Patton J.L., 1976. Karyotypic variation in oryzomyine rodents (Cricetinae) with comments on chromosomal evolution in the Neotropical cricetine complex. Occ. Pap. Mus. Zool., La. State Univ. 49: 1–47.

González-Ittig, R.E., Salazar-Bravo J., Barquez R.M., Gardenal C.N., 2010. Phylogenetic relationships among species of the genus *Oligoryzomys* (Rodentia, Cricetidae) from Central and South America. Zool. Scr. 39: 511–526.

González-Ittig R.E., Rivera P.C., Levis S.C., Calderón G.E., Gardenal C. N., 2014. The molecular phylogenetics of the genus *Oligoryzomys* (Rodentia: Cricetidae) clarifies rodent host–hantavirus associations. Zool. J. Linn. Soc. 171 (2): 457–474.

Guterres A., de Oliveira R.C., Fernandes J., Schrago C.G., de Lemos E.R.S., 2015. Detection of different South American hantaviruses. Virus Res. 210: 106–113. doi:10.1016/j.virusres.2015.07.022.

Hall T.A., 1999. BioEdit: a user-friendly biological sequence alignment editor and analysis program for Windows 95/98/NT. Nucleic Acids Symp. Ser. 41: 95–98.

Hanson J.D., 2008. Molecular phylogenetics of the tribe Oryzomyini: does a multi-gene approach help resolve a systematic conundrum? Ph.D. Thesis, Texas Tech University, Lubbock, Tx.

Hanson J.D., A. Utrera, Fulhorst C.F., 2011. The delicate pygmy rice rat (*Oligoryzomys delicatus*) is the principal host of Maporal Virus (Family Bunyaviridae, Genus Hantavirus). Vector-Borne and Zoonotic Dis. 11(6): 691–696.

Hershkovitz P., 1966. South American Swamp and fossorial rats of the Scapteromyine group (Cricetinae, Muridae), with comments on the glans penis in murid taxonomy. Z. Säugetierk. 31: 81–149.

Holm S., 1979. A simple sequential rejective multiple test procedure. Scand. J. Stat. 6: 65–70.

Huelsenbeck J.P., Ronquist F., Nielsen R., Bollback J.P., 2001. Bayesian inference of phylogeny and its impact on evolutionary biology. Science 294: 2310–2314.

Hurtado N., 2021. A new species of the genus *Oligoryzomys* (Rodentia: Cricetidae) from Peru. J. Mammal. 102(3): 931–946. doi:10.1093/jmammal/gyab030.

Hurtado N., and D'Elía G., 2018. A new species of long-tailed mouse, genus *Oligoryzomys* Bangs, 1900 (Rodentia: Cricetidae), from the Bolivian Yungas. Zootaxa 4500(3): 341–362. doi:10.11646/zootaxa.4500.3.3.

Hurtado N., D'Elía G., 2019. An assessment of species limits of the South American mouse genus *Oligoryzomys* (Rodentia, Cricetidae) using unilocus delimitation methods. Zool. Scr. 48(5): 557–570.

Hurtado, N., and D'Elía, G. 2022. Historical biogeography of a rapid and geographically wide diversification in Neotropical mammals. J. Biogeog. 49(5): 781–793.

Irwin D.M., Kocher T.D., Wilson A.C., 1991. Evolution of the cytochrome b gene of mammals. J. Mol. Evol. 32: 128–144.

Janiak M.C., Silva F.E., Beck R.M.D., Vries D. de, Kuderna L.F.K., Torosin N.S., Melin A.D., Marquès- Bonet T., Goodhead I.B., Messias M., da Silva M.N..F, Sampaio I., Farias I.P., Rossi R., Melo F.R. de, Valsecchi J., Hrbek T., Boubli J.P., 2022. Two hundred and five newly assembled mitogenomes provide mixed evidence for rivers as drivers of speciation for Amazonian primates. Mol. Ecol. 31: 3888-3902. https://doi.org/10.1111/mec.16554

Josse J., Husson F., 2016. missMDA: A Package for Handling Missing Values in Multivariate Data Analysis. Journal of Statistical Software 70(1): 1–31. doi:10.18637/jss.v070.i01.

King M., 1993. Species evolution: the role of chromosome change. Cambridge University Press, Cambridge.

Kozlov A.M., Stamatakis, A., 2019. Using RAxML-NG in Practice. Preprints.org, 2019050056. https://doi.org/10.20944/preprints201905.0056.v1.

Lima J.F.S., 2004. Diversidade cariológica de roedores de pequeno porte do estado de Tocantins. PhD thesis, Instituto de Biociências, Universidade Estadual de São Paulo, Rio Claro, Brazil.

Machado L.F., Paresque R., Christoff A.U., 2011. Anatomia comparada e morfometria de *Oligoryzomys nigripes* e *O. flavescens* (Rodentia, Sigmodontinae) no Rio Grande do Sul, Brasil. Pap. Avulsos Zool. (São Paulo) 51(3): 29-47. doi:10.1590/S0031-10492011000300001.

Machado L.F., Leite Y.L., Christoff A.U., Giugliano L.G., 2014. Phylogeny and biogeography of tetralophodont rodents of the tribe Oryzomyini (Cricetidae: Sigmodontinae). Zool. Scr. 43: 119–130.

Matocq M.D., Shurtliff Q.R., Feldman, C.R., 2007. Phylogenetics of the woodrat genus *Neotoma* (Rodentia: Muridae): Implications for the evolution of phenotypic variation in male external genitalia. Mol. Phylogen. Evol. 42(3): 637–652. doi:10.1016/j.ympev.2006.08.011.

McCarthy C., 1998. Chromas version 1.45 (32-bit).

Milazzo M. L., Cajimat M.N., Hanson J.D., Bradley R.D., Quintana M., Sherman C., Velásquez R.T., Fulhorst C.F., 2006. Catacamas virus, a hantaviral species naturally associated with *Oryzomys couesi* (Coues' oryzomys) in Honduras. Am. J. Trop. Med. Hyg. 75: 1003–1010.

Miller M.A., Pfeiffer W., Schwartz T., 2010. Creating CIPRES Science Gateway for inference of large phylogenetic trees. Proceedings of the Gateway Computing Environments Workshops (GCE), New Orleans, La., 1–8.

Mull N., Jackson R., Sironen T., Forbes K.M., 2020. Ecology of neglected rodent-borne American orthohantaviruses. Pathogens 9(5): 325. doi:10.3390/pathogens9050325.

Myers P., Carleton M.D., 1981. The species of *Oryzomys* (*Oligoryzomys*) in Paraguay and the identity of Azara's "rat sixieme ou rat à tarse noir". Misc Publ. Mus. Zool. Univ. Mich. 161:1–41.

Naka L.N., da Silva Costa B.M., Lima G.R., Claramunt S., 2022. Riverine Barriers as Obstacles to Dispersal in Amazonian Birds. Front. Ecol. Evol. 10: 84697.

Nikulin A., 2020. Proto-Macro-Jê: um estudo reconstrutivo. PhD Thesis, Departamento de Linguística, Português e Línguas Clássicas, Universidade de Brasília, Brasília, Brazil.

Nunes M.L., Oliveira S.V. de, Elkhoury M. da R., Fonseca L.X., Pereira S.V.C., Caldas E.P., Guimarães J.C.N., Rosa E.S.T., Bonvicino C.R., D'Andrea, P.S., 2015. Evidência de circulação de hantavirus em área silenciosa da Região Amazônica. Rev. Pan-Amaz. Saude 6(4): 63–67. doi:10.5123/S2176-62232015000400009.

Ojeda, A.A., Teta, P., Pablo Jayat, J., Lanzone, C., Cornejo, P., Novillo, A., Ojeda, R.A., 2021. Phylogenetic relationships among cryptic species of the *Phyllotis xanthopygus* complex (Rodentia, Cricetidae). Zool. Scr. 50(3): 269–281. doi:10.1111/zsc.12472.

Oliveira J.A., Strauss R.E., Reis S.F., 1998. Assessing relative age and age structure in natural populations of *Bolomys lasiurus* (Rodentia: Sigmodontinae) in Northeastern Brazil. J. Mammal. 79: 1170–1183.

Oliveira R.C, Teixeira B.R., Mello F.C., Pereira A.P., Duarte A.S., Bonaldo M.C., Bonvicino C.R., D'Andrea P.S., de Lemos E.R.S., 2009. Genetic characterization of a Juquitiba-like viral lineage in *Oligoryzomys nigripes* in Rio de Janeiro, Brazil. Acta Tropica 112: 212–318.

Oliveira R.C., Padula P.J., Gomes R., Martinez V.P., Bellomo C., Bonvicino C.R., Freire e Lima D.I., Bragagnolo C, Caldas A.C.S, D'Andrea P.S, de Lemos E.R.S., 2011. Genetic characterization of hantaviruses associated with sigmodontine rodents in an

endemic area for hantavirus pulmonary syndrome in southern Brazil. Vector Borne Zoonotic Dis. 11: 301–314.

Oliveira R.C., Guterres A., Fernandes J., D'Andrea P.S., Bonvicino C.R., de Lemos E.R.S., 2014. Hantavirus reservoirs: current status in the world with an emphasis on data from Brazil. Viruses 6(5): 1929–1973.

Oliveira da Silva W., Rosa C.C., Ferguson-Smith M.A., O'Brien P.C.M., Saldanha J., Rossi R.V., Pieczarka J.C., Nagamachi C.Y. 2022. The emergence of a new sex-system (XX/XY1Y2) suggests a species complex in the "monotypic" rodent *Oecomys auyantepui* (Rodentia, Sigmodontinae). Sci. Rep. 12(1): 8690. doi:10.1038/s41598-022-12706-3.

Palma R.E., Cancino R.A., Rodríguez-Serrano E., 2010a. Molecular systematics of *Abrothrix longipilis* (Rodentia: Cricetidae: Sigmodontinae) in Chile. J. Mammal. 91: 1102–1111.

Palma R.E., Rivera-Milla E., Salazar-Bravo J., Torres-Pérez F., Pardiñas U.F.J., Marquet P.A., Spotorno A.E., Meynard A.P., Yates T. 2005. Phylogeography of *Oligoryzomys longicaudatus* (Rodentia: Sigmodontinae) in temperate South America. J. Mammal. 86(1): 191–200.

Palma R.E., Rodríguez-Serrano E., Rivera-Milla E., Hernandez C.E., Salazar-Bravo J., Carma M.I., Belmar-Lucero S., Gutierrez-Tapia P., Zeballos H., Yates T.L., 2010b. Phylogenetic relationships of the pygmy rice rats of the genus *Oligoryzomys* Bangs, 1900 (Rodentia, Sigmodontinae). Zool. J. Linnean Soc. 160: 551–566.

Patton J.L., M.N.F. da Silva., 1995. A review of the spiny mouse genus *Scolomys* (Rodentia: Muridae: Sigmodontinae) with the description of a new species from the western Amazon of Brazil. Proc. Biol. Soc. Washington 108 (2): 319–337.

Patton J.L., M.N.F. da Silva., 1998. Molecular phylogeography and the evolution and conservation of Amazonian mammals. Mol. Ecol. 7(4): 475-86.

Patton J.L., da Silva M.N.F., Malcolm J.R., 2000. Mammals of the Rio Juruá and the evolutionary and ecological diversification of Amazonia. Bull. Am. Mus. Nat. Hist. 244: 1–306.

Percequillo A.R., Weksler M., Costa L.P., 2011. A new genus and species of rodent from the Brazilian Atlantic Forest (Rodentia: Cricetidae: Sigmodontinae: Oryzomyini), with comments on oryzomyine biogeography. Zool. J. Linnean Soc. 161 (2): 357–390.

Pereira L.G., Geise L., 2007. Karyotype composition of some rodents and marsupials from Chapada Diamantina (Bahia, Brazil). Braz. J. Biol. 67(3): 509–518.

Powers A.M., Mercer D.R., Watts D.M., Guzman H., Fulhorst C.F., Popov V.L., Tesh R.B., 1999. Isolation and genetic characterization of hantavirus (Bunyaviridae: Hantavirus) from a rodent, *Oligoryzomys microtis* (Muridae), collected in northeastern Peru. Am. J. Trop. Med. Hyg. 61: 92–98.

Quiroga-Carmona M., Abud C., Lessa E.P., D'Elía G., 2022. The mitochondrial Genetic diversity of the Olive Field Mouse *Abrothrix olivacea* (Cricetidae; Abrotrichini) is latitudinally structured across its geographic distribution. J. Mammal. Evol. 29(2): 413–430. doi:10.1007/s10914-021-09582-5.

Rambaut A., Drummond A., 2007. Tracer v1.4. http://beast.bio.ed.ac.uk/Tracer

Reig O.A., 1977. A proposed unified nomenclature for the enamelled components of the molar teeth of the Cricetidae (Rodentia). J. Zool. 181: 227–241.

Ribas C., Aleixo A., Nogueira A., Miyaki C., Cracraft J., 2011. A paleobiogeographic model for biotic diversification within Amazonia over the past three million years.

Proceedings of the Royal Society B 279(1729):681–689. doi: 10.1098/rspb.2011.1120

Rice W., 1989. Analyzing tables of statistical tests. Evolution 43: 223–225.

Richter M.H., Hanson J.D., Cajimat M.N., Milazzo M.L., Fulhorst C.F., 2010. Geographical range of Rio Mamore virus (family Bunyaviridae, genus *Hantavirus*) in association with the small-eared pygmy rice rat (*Oligoryzomys microtis*). Vector Borne Zoonotic Dis. 10: 613–620.

Ridgway, R., 1912. Color standards and color nomenclature. The author, Washington.

Ripley B., Venables B., Bates D.M., Hornik K., Gebhardt A., Firth D., Ripley M.B. 2013. Package 'mass.' Cran r 538: 113–120.

Rivera P.C., González-Ittig R.E., Fraire H.J.R., Levis S. Gardenal C.N., 2007. Molecular identification and phylogenetic relationships among the species of the genus *Oligoryzomys* (Rodentia, Cricetidae) present in Argentina, putative reservoirs of hantaviruses. Zool. Scripta. 36(3): 231–239. doi:10.1111/j.1463-6409.2007.00273.x.

Rivera P.C., González-Ittig R.E., Robainas Barcia A., Trimarchi L.I., Levis S., Calderón G.E., Gardenal C.N., 2018. Molecular phylogenetics and environmental niche modeling reveal a cryptic species in the *Oligoryzomys flavescens* complex (Rodentia, Cricetidae). J. Mammal. 99(2): 363–376. doi:10.1093/jmammal/gyx186.

Rocha R.G., Ferreira E., Costa B., Martins I., Leite Y.L., Costa L.P., Fonseca C., 2011. Small mammals of the mid-Araguaia River in central Brazil, with the description of a new species of climbing rat. Zootaxa 2789: 1–34.

Rodríguez F., Oliver J.L., Marín A., Medina J.R., 1990. The general stochastic model of nucleotide substitution. J. Theoret. Biol. 142: 485–501.

Rogers D.S., Arenas E.A., González-Cózatl F.X., Hardy D.K., Hanson J.D., Lewis-Rogers N., 2009. Molecular phylogenetics of *Oligoryzomys fulvescens* based on

cytochrome b gene sequences, with comments on the evolution of the genus *Oligoryzomys*. In: F.A. Cervantes (Eds.) 60 años de la Colección Nacional de Mamíferos del Instituto de Biología, UNAM. Aportaciones al Conocimiento y Conservación de los Mamíferos Mexicanos. Universidad Autonoma de México, D.F., México. 209–222.

Ronquist F., Huelsenbeck J.P., 2003. MrBayes 3: Bayesian phylogenetic inference under mixed models. Bioinformatics 19: 1572–1574.

Rosa E.S.T., Mills J.N., Padula P.J., Elkhoury M.R., Ksiazek T.G., Mendes W.S., Santos E.D., Araujo G.C., Martinez V.P., Rosa J.F., Edelstein A., Vasconcelos P.F.C., 2005. Newly recognized hantaviruses associated with hantavirus pulmonary syndrome in northern Brazil: partial genetic characterization of viruses and serologic implication of likely reservoirs. Vector Borne Zoonotic Dis. 5: 11–19.

Rosa E.S.T., de Lemos E.R.S., Medeiros D.B.A., Simith D.B., Pereira A.S., Elkhoury M.R., Mendes W.S., Vidigal J.R., Oliveira R.C., D'Andrea P.S., Bonvicino C.R., Cruz A.C., Nunes M.R., Vasconcelos P.F.C., 2010. Hantaviruses and hantavirus pulmonary syndrome, Maranhão, Brazil. Emerging Infect. Dis. 16: 1952–1955.

Rosa E.S.T., Medeiros D., Nunes M.R., Simith D.B., Pereira A.S., Elkhoury M.R., Nunes M.R., Marques A., Via A., D'Andrea P.S., Bonvicino C.R., de Lemos E.R.S., Vasconcelos P.F.C., 2011. Pygmy rice rat as potential host of Castelo dos Sonhos Hantavirus. Emerging Infect. Dis. 17(8): 1527–1530.

Sambrook J., Russell D.W., 2001. Molecular Cloning: A Laboratory Manual. Cold Spring Harbor Laboratory Press, Cold Spring Harbor, NY.

Santorelli S., Magnusson W.E., Deus C.P., 2018. Most species are not limited by an Amazonian river postulated to be a border between endemism areas. Sci. Rep. 8: 2294. https://doi.org/10.1038/s41598-018-20596-7

Sbalqueiro I.J., Mattevi M.S., de Oliveira L.F.B., Solano M.J.V., 1991. B chromosome system in populations of *Oryzomys flavescens* (Rodentia, Cricetidae) from southern Brazil. Acta Theriol. 36: 193–199.

Sikes, R.S. and the Animal Care and Use Committee of the American Society of Mammalogists, 2016. 2016 Guidelines of the American Society of Mammalogists for the use of wild mammals in research and education: J. Mammal. 97(3): 663–688. doi:10.1093/jmammal/gyw078.

Smith M.F., Patton J.L., 1993. The diversification of South American murid rodents: evidence from mitochondrial DNA sequence data for the akodontine tribe. Biol. J. Linnean Soc. 50: 149–177.

Sokal R.R., Rohlf F.J., 1994. Biometry: The principles and practice of statistics in biological research. W. H. Freeman, New York, NY.

Strauss, R.E., 2010. Discriminant groups of organisms. In: Elewa A.M.T. (Ed.) Morphometrics for Nonmorphometricians (Lecture Notes in Earth Sciences vol. 124). Springer-Verlag, Berlin. 73–91.

Suzuki A., Bisordi I., Levis I., Garcia J., Pereira P.E., Souza R.P., Sugahara T.K., Pini N., Enria D., Souza L.T., 2004. Identifying Rodent Hantavirus Reservoirs, Brazil. Emerging Infect. Dis. 10: 2127–2134.

Swofford D.L., 2002. PAUP*. Phylogenetic Analysis Using Parsimony (*and Other Methods), v. 4.0. Sinauer Associates, Sunderland, Ma.

Teta P., Jayat J.P., Ortiz P.E., D'Elía G., 2013. The taxonomic status of *Oligoryzomys brendae* Massoia, 1998 (Rodentia, Cricetidae), with comments on the availability of this name. Zootaxa, 3641(4): 433–447.

Vidal-Rioja L., Fronza T.G. de, Wainberg R., Brum-Zorilla N., Wallace F., Zambelli A., 1988. C-banding pattern and satellite DNA localization on the chromosomes of

Oryzomys flavescens (Rodentia, Cricetidae). Caryologia 41: 323–328. DOI:10.1080/00087114.1988.10797872.

Villalobos-Dominguez, C., Villalobos, J., 1947. Atlas de los Colores. (Colour Atlas). With 7,279 illustrations on 38 colour plates. El Ateneo, Buenos Aires.

Voss, R.S., 1988. Systematics and ecology of ichthyomyine rodents (Muroidea): patterns of morphological evolution in a small adaptive radiation. Bull. Am. Mus. Nat. Hist. 188: 260–493.

Voss R.S., Lunde D.P., Simmons, N.B., 2001. The mammals of Paracou, French Guiana: A neotropical lowland rainforest fauna. Part 2. Nonvolant species. Bull. Am. Mus. Nat. Hist. 263: 1–236.

Wallace A.R., 1853. On the monkeys of the Amazon. Ann. Mag. Nat. Hist. 14(3): 451 – 454. DOI: https://doi.org/10.1080/037454809494374

Weksler M., 2006. Phylogenetic relationships of oryzomine rodents (Muroidea, Sigmodontinae): separate and combined analyses of morphological and molecular data. Bull. Am. Mus. Nat. Hist. 296: 1–149.

Weksler M., Bonvicino C.R., 2005. Taxonomy of pigmy rice rats genus *Oligoryzomys* Bangs, 1900 (Rodentia, Sigmodontinae) of the Brazilian Cerrado, with the description of two new species. Arquivos Mus. Nac. 63: 113–130.

Weksler M., Bonvicino C.R., 2015. Genus *Oligoryzomys* Bangs. In Patton J.L., Pardiñas U.F.J., D'Elía G. (Eds.) Mammals of South America. Volume 2 Rodents. University of Chicago Press, Chicago, Il. 417– 437.

Weksler M., de Lemos E.M.S., D'Andrea P.S., Bonvicino, C.R. 2017., The Taxonomic status of *Oligoryzomys mattogrossae* (Allen 1916) (Rodentia: Cricetidae: Sigmodontinae), reservoir of Anajatuba Hantavirus. Amer. Mus. Novitates 3880(3880): 1–32. doi:10.1206/3880.1.

Yang, Z. 1994. Maximum likelihood phylogenetic estimation from DNA sequences with variable rates over sites: approximate methods. J. Mol. Evol. 39: 306–314.

Figure legends

Figure 1. Map showing the collection localities of *O. microtis* (black symbols), and *Oligoryzomys* sp. n. (grey and white symbols). Stars correspond to type localities. Numbers refer to localities listed in appendices 1 and 2 and table 1.

Figure 2. Karyotypes in conventional coloration of (A) *O. microtis* topotype male MN84349 with 2n=64 and FN=66, (B) *Oligoryzomys* sp. n. female MN91085 from Central clade (Rondônia, Brazil), with 2n=64 and FN=64, (C) *O. mattogrossae* male CRB3141 from Brasília, Brazil with 2n=62 and FN=64, and (D) *Oligoryzomys* sp. n. female MN81643 from Eastern clade (Tocantins, Brazil) with 2n=64 and FN=64.

Figure 3. Phylogenetic relationships among *Oligoryzomys* specimens based on maximum likelihood analysis of mt-Cytb**.** Bootstrap values (bs, %) are shown above branches; posterior probabilities of Bayesian analysis are shown below branches. Locality numbers for *O. microtis* and *Oligoryzomys* sp. n. are in parentheses; diploid number (2n) and fundamental number (FN) are based on karyotyped specimens marked in bold; specimens that were reported positive for virus-specific RNA *Orthohantavirus* are marked with asterisks: * for RIOMV strain (Bharadwaj et al. 1997; Carroll et al. 2005); ** for strain HTN-007 (Powers et al. 1999; Oliveira et al. 2014); *** for RIOMV-3 (Firth et al. 2012); and **** for RIOMV-4 (Firth et al. 2012). See appendix 2 for outgroups and specimen information.

Figure 4. (A) Median joining network within *O. microtis* and *Oligoryzomys* sp. n. Circles are haplotypes proportional to number of sequences; small black circles are median

vectors (hypothetical haplotypes); small bars indicate nucleotide substitutions; numbers refer to haplotype numbers listed in appendix 3; see legend for geographic source of haplotypes. (B) Pairwise uncorrected (´p´) genetic distances for three contrasts: within species, between clades of *Oligoryzomys* sp. n. and between species.

Figure 5. Combined violin and box plots for external measurements of *Oligoryzomys microtis* complex. Violin plot shows kernel density plot from minimum to maximum value. The box plot shows the median, 25-75 percent quartiles (boxes), values less or more than 1.5 times the box height (whiskers), and outliers. Measurements are: (A) HBL: head-and-body length, (B) TL: tail length, (C) HF: hind-feet length, and (D) Ear: ear length. Lines above each graph show significant differences among groups: ** < 0.01, *** < 0.001.

Figure 6. Dorsal, lateral and ventral views of skins of *Oligoryzomys* sp. n. from Eastern clade (Tocantins State, MN76206), *Oligoryzomys* sp. n. from Central clade (Rondônia State, MN87921), and *O. microtis* (Acre State, MN87929).

Figure 7. Dorsal, ventral, and lateral views of the skull of *Oligoryzomys* sp. n. from Central clade (Rondônia State, MN87921), *Oligoryzomys* sp. n. from Eastern clade (Tocantins State, MN76206).

Figure 8. Comparative plate of *Oligoryzomys* skulls, showing the variation of six selected qualitative traits: depth of the zygomatic notch (dorsal view; A-B), interorbital region (dorsal view, C-D), width of interparietal (dorsal view, E-F), presence of jugal (lateral view; G-H), and shape of incisive foramina and length of palate (ventral view; I-K). (A)

Oligoryzomys sp. n., Central clade (MN87906); (B, D, F, H, I) *O. microtis* (MN87951); (C) *Oligoryzomys* sp. n., Central clade (MN87901); (E, G, K) *Oligoryzomys* sp. n., Eastern clade (MN76227); (J) *Oligoryzomys* sp. n., Central clade (MN87907).

Figure 9. Principal component (A-D) and canonical discriminant (E-H) analyses of log-transformed cranial measurements. Scatterplots A and E include all analyzed specimens, while remaining graphs refer to pairwise contrasts between: (B and F) eastern and Central clades of *Oligoryzomys* sp. n., (C and G) *O. microtis* and Eastern clade of *Oligoryzomys* sp. n., and (D and H) *O. microtis* and Central clade of *Oligoryzomys* sp. n..

Supplementary figure 1. Phylogenetic relationships among *Oligoryzomys* specimens based on maximum likelihood analyses of combined mt-Cytb and i7FGB. See appendix 2 for outgroups and specimen information.

Supplementary figure 2. Summarized variation in six qualitative characters among *O. microtis* and *Oligoryzomys* sp. n. (Central and Eastern clades): Zygomatic notch and plate, interorbital region, interparietal width, jugal presence, incisive foramina shape, and palate length. Sample size is given between parentheses.

Appendix 1. List of *O. microtis* and *Oligoryzomys* sp. n. specimens analyzed, specifying the markers sequenced I7bg (^{i7}), mt-Cytb (^{cy}), cytochrome oxidase 1 (^{coi}) and/or individuals karyotyped (^{k}) or measured (^{m}). Because several specimens listed in GenBank are referred by their field numbers, these are provided in parenthesis, when available. Additional specimens employed in phylogenetic analyses but not morphologically or cytogenetically analyzed by us are listed in appendix 2. Mammals' collections acronyms are: MN (Museu Nacional, UFRJ, Brazil), LBCE (ColMasto, Fiocruz, Brazil), USNM (United States National Museum, USA), AMNH (American Museum of Natural History, USA). Collector acronyms are: CRB (Cibele Rodrigues Bonvicino), FO (Fazenda Osara), PQ (Pequizeiro), SVS (Serviço de Vigilância em Saúde, Ministry of Health, Brazil). Numbers in parentheses refer to sampling localities in map (fig. 1).

Oligoryzomys sp. n. Central clade:

BRAZIL, Mato Grosso state, **(1) Alta Floresta**: MN89726^{k,m} (SVS1028), MN87938^{m} **(**SVS1048); **Rondônia state**, **(7) Alto Paraíso, Fazenda do Sr. Bento**: MN91084^{i7,cy,k} (LBCE7038/SVS003), MN91085^{cy,k} (LBCE7039/SVS004), SVS005, MN87897 (SVS006), SVS007, SVS009, SVS010, SVS011, SVS017^{i7}, MN87898 (SVS018), SVS019, SVS020, LBCE20448^{i7} (SVS021), SVS022-SVS024, SVS027, SVS028, MN87899 (SVS030), MN87900 (SVS031), SVS032, MN87901 (SVS034), MN87902^{m} (SVS037), SVS038, SVS040-SVS043, MN87903^{m} (SVS047), SVS049, SVS051, MN87904^{m} (SVS053), MN91083 (SVS055), MN87905^{m} (SVS056), SVS057, SVS058, SVS060, SVS061, LBCE20474^{i7} (SVS062), MN87906^{m} (SVS063), SVS064, MN87907 (SVS067), SS068, SVS069, SVS072, MN87908^{m} (SVS0073), MN87909^{m} (SVS0074), LBCE20483^{i7} (SVS075), SVS076, MN87910^{m} (SVS077), MN87911^{m} (SVS078),

MN87912[m] (SVS079), MN87913[m] (SVS081), MN87914[m] (SVS082), MN87915[m] (SVS083), MN87916[m] (SVS084), MN87916[m] (SVS087), MN87917[m] (SVS089), SVS092, LBCE20492[i7] (SVS093), MN87918[m] (SVS099), SVS106[cy], MN91086[m] (SVS107), SVS108[cy], SVS113, SVS116, SVS117, MN87919[cy,m] (SVS118), MN87920[m] (SVS127), SVS129, MN87921[cy,m] (LBCE 20531/SVS134).

Oligoryzomys sp. n. Eastern clade:

BRAZIL, Pará state, **Belem, (2) Utinga:** MN91079[m], MN91080 [m], USNM461070[m] USNM461071[m] USNM461076[m]; **Marabá, (3) 73 Km N And 45 Km W, Near Jatobal:** USNM519769[m], USNM519770[m] USNM521454[m], USNM521455[m], USNM521456[m], USNM521457[m], USNM521458[m], USNM521459[m], USNM521460[m], USNM521461[m], USNM521462[m], USNM521540[m]; **Marabá, (4) Floresta Nacional de Tapirapé-aquiri**: MN75541, MN75575; **Parauapebas, (5) Floresta Nacional de Carajás:** MN73863, MN73978, MN75447, MN91082; **(6) Itupiranga**, **Programa Assentamento Benfica 1:** LBCE6722[k], **Tocantins state**, **São Sebastião do Tocantins, (8) Fazenda Osara II**: MN76192[m,coi] (FO05), MN76194[m,k,coi] (FO07), MN76198[m,k,coi] (FO10), MN76200[m] (FO13), MN76203[m] (FO16), MN75205[k,coi] (FO18), MN76206[m,coi] (FO19), MN76207[m,coi] (FO20), MN76209[m,coi] (FO22), MN76210[m,k,coi] (FO23), MN76212[m,k,coi] (FO25), MN76213[m,coi] (FO26), MN76216[m,coi] (FO29), MN76217[m,coi] (FO30), MN76223[m,k,coi] (FO36), MN81726 (FO41), MN76226[m] (FO43), MN81727 (FO44), MN76227[m] (FO45), MN80436 (FO47), MN80431 (FO39), MN81639[i7,cy] (offspring of MN81726), MN81640[k] (offspring of MN81726), MN81641[k,i7] (offspring of MN81727), MN81642[i7] (offspring of MN81727), MN81643[k,i7] (offspring of MN81726), MN81646 (born in captivity); **Couto Magalhães, (9) Fazenda do Zé Carlos**: MN76925[m,k,coi] (PQ23), MN76926[m,k,coi] (PQ24).

Oligoryzomys microtis

BOLIVIA, El Beni, (12) Boroica, Rio Itonama: USNM460740[m]; **(13) Cachuelita, Itonama, Rio S. Huios, Las Petas**: USNM460739[m]; **(14) Chaco Lejo, 20 Km SE San Ramon**: USNM391295[m] USNM391296[m] USNM391297[m]; **(15) Las Penas, Rio Machupo**: USNM460741[m]; **(16) San Joaquin**: USNM364738[m] USNM391299[m] USNM460273[m] USNM460742[m] USNM460743[m]. **BRAZIL, Acre state, (17) Brasiléia**: LBCE13098[k,cy], **(18) Capixaba:** MN87922[cy] (SVS638), MN87923[cy] (SVS639), MN87924[cy,m] (SVS641), MN87925[cy,m] (SVS642), MN87926[cy] (SVS643), MN87927[cy,m] (SVS645), SVS647[cy], MN87928[cy] (SVS650), MN87929[cy,m] (SVS663), MN87930[cy] (SVS665), MN87931[cy] (SVS666), MN89725[cy] (SVS673), MN87932[cy] (SVS675), SVS676[cy], MN87933[m] (SVS680), SVS689[cy], MN87934[m] (SVS706), SVS712[cy], MN87937[m] (SVS723); **Porto Acre, (19) Humaitá:** MN87950[cy,m] (LBCE18369), MN87951[cy,k,m] (LBCE18385), MN87953[k] (LBCE18403); **Porto Acre, Rodovia AC10, Km20, (20) Ramal Prof[a] Lucila:** MN87939[m] (LBCE15118), LBCE15123[k,cy], MN87942[m] (LBCE15124), LBCE15126[k,cy], MN87945[m] (LBCE15132), MN87946[m] (LBCE15133), LBCE 15135[k,cy], MN87948[m] (LBCE15136), LBCE15141[k,cy]; **(21) Rio Branco, Parque Zoobotânico:** MN87952[cy,m] (LBCE18400), LBCE18403[m]; **Amazonas state**, **(22) Manacapuru, Paraíso D'Angelo:** MN84349[cy,k] (CRB3004); **Solimões River (restricted by Voss et al. 2001 to Manacapuru)**: AMNH37091[m], AMNH37096[m], AMNH37157[m]; **PERU, Madre de Dios, Tambopata, (23) Puerto Maldonado**: USNM390112[m], USNM390115[m], USNM390116[m], USNM390117[m], USNM390118[m], USNM390119[m]; **(24) Rio Manu, 57 Km Above Mouth**: USNM559399[m], USNM559400[m], USNM559401[m], USNM559402[m], USNM559403[m]; **(25) Rio Tambopata, 30 Km From Mouth**: USNM530925[m], **Ucayali, (26) 59 Km SW Pucallpa**: USNM499223[m], USNM499224[m].

Appendix 2. Specimens used in molecular analysis. Museum and collector acronyms are: ACUNH (Abilene Christian University Natural History, Texas, USA), AMNH (American Museum of Natural History, New York, USA), AN (Instituto Evandro Chagas, Ananindeua, Brazil) ASNHC (Angelo State Natural History Collections, San Angelo, TX, USA), Bar (Bariloche, specimens at Instituto Nacional de Enfermedades Virales Humanas, Pergamino, Buenos Aires, Argentina), AVG (unknown field number, specimens at MUSM), BYU (Monte L. Bean Museum, Brigham Young University, Provo, UT, USA), CIT (Laboratório de Citogenética de Vertebrados, Universidade de São Paulo, Brazil), (Carnegie Museum of Natural History, Pittsburgh, PA, USA), CNP (Campo Novo do Parecis), CRB (Cibele Rodrigues Bonvicino), CURN (Centro Universitario Regional del Norte de la Universidad Autónoma de Nicaragua), GD (Guillermo D´Elía), IMBICE (Instituto Multidisciplinario de Biologia Celular, La Plata, Argentina), INEVH *(*Instituto Nacional de Enfermedades Virales Humanas "Dr. Julio I. Maiztegui," Buenos Aires, Argentina), JMR (José M. Rojas), (Colección de Mamíferos del Centro Nacional Patagonico, Puerto Madryn, Argentina), LBCE (ColMasto, FIOCRUZ, Rio de Janeiro, Brazil), LF (Luís Flamarion), MACN (Museo Argentino de Ciencias Naturales "Bernardino Rivadavia," Buenos Aires, Argentina), MCNU (Museu de Ciencias Naturais da Ulbra, Brazil), MN (Museu Nacional, Universidade Federal do Rio de Janeiro, Brazil), MNFS (Maria Nazaré F. da Silva), MPEG (Museu Paraense Emílio Goeldi, Belém, Pará, Brazil), MSB (Museum of South western Biology, University of New Mexico, Albuquerque, USA), MUSM (Museo de Historia Natural, Universidade Mayor de San Marcos, Lima, Peru), MVZ (Museum of Vertebrate Zoology, University of California, Berkeley, USA), NK (Museum of Southwestern Biology, University of New Mexico, Albuquerque, USA), OMNH (Sam Noble Museum, University of Oklahoma, Norman, USA), JPJ (Jorge Pablo Jayat), ROM (Royal Ontario Museum, Ottawa, Canada), RCO (unknown field number, specimens at

MUSM), SVS (Serviço de Vigilância em Saúde, Ministry of Health, Brazil), TK (Tissue collection, Texas Tech University, Lubbock, TX, USA), TTU (The Museum, Texas Tech University, Lubbock, TX, USA), UFES (Universidade Federal do Espírito Santo, Vitória, Brazil), UFPB (Universidade Federal da Paraíba, João Pessoa, Brazil), UNB (Universidade de Brasília, Distrito Federal, Brazil). References (Ref.) for sequences are: 1= Hurtado and D'Elía 2019, 2= Hurtado and D'Elía 2022, 3= Teta et al. 2013, 4= González-Ittig et al. 2010, 5= Hanson et al. 2011, 6= Percequillo et al. 2011, 7= Milazzo et al. 2006, 8= Hurtado and D'Elía 2 8, 9= Agrellos et al. 2012, 10= González-Ittig et al. 2014, 11= Palma et al. 2005, 12=Weksler et al. 2017, 13=Rogers et al. 2009, 14= da Cruz et al. 2019, 15= Palma et al. 2010b, 16=Firth et al. 2012, 17= Rocha et al. 2011 18= Carroll et al. 2005, 19= Patton and Silva 1995, 20= Richter et al. 2010, 21= Palma et al. 2010a, 22=Canon et al. 2014, 23=Smith and Patton 1999, 24=Hanson 2008, 25= Bonvicino et al. 2014, 26= Almendra et al. 2014, 27=Machado et al. 2014, 28= D'Elía et al. 2015, 29= Oliveira da Silva et al. 2022, PS= present study, Unp.= unpublished.

Taxon	Locality	Voucher Number	mt-Cytb	ifgb7	Ref. mt-Cytb	Ref. Ifgb7
O. andinus	Peru: Huánuco, Huamalíes, Punchao, Chinchuragra	MUSM22887	MK128667	MW390661	1	2
O. andinus	Peru: Lima, Huaura, Huacho, Albúferas Medio Mundo	MUSM42033	MK128685	MW390662	1	2
O. arenalis	Peru: Piura, Huancabamba, Canchaque, Chorro Blanco	MUSM21694	MK128692	MW390665	1	2

Taxon	Locality	Voucher Number	mt-Cytb	ifgb7	Ref. mt-Cytb	Ref. Ifgb7
O. arenalis	Peru: Cajamarca, Chota, Querocoto, Quebrada Honda	MUSM39523	MK128695	MW390666	1	2
O. brendae	Argentina: Jujuy, Quebrada Alumbriojo, aprox. 8 km al NE de Santa Ana	JPJ2219	JX154134	MW390668	3	2
O. brendae	Argentina: La Rioja, Km 14 de la ruta provincial N° 73, aprox. 1 km de Pampa de la Viuda	JPJ2423	JX154133	MW390667	3	2
O. chacoensis	Argentina: Salta	INEVH-Or22498	GU185904	-	4	-
O. chacoensis	Paraguay: Presidente Hayes, Estancia Loma Pora	TTU118460/TK62086	MK128704	MW390669	1	2
O. chacoensis	Paraguay: Boqueron, La Lomita, Base Naval Pedro P. Peña	TTU104514	-	MW390670	-	2
O. costaricensis	Panama: Los Santos	MSB96068/NK101603	MK128706	MW390672	1	2
O. costaricensis	Panama: Gamboa	TK163369	GU393988	-	5	-
O. costaricensis	Costa Rica: Cartago, 2 km NE Cartago	MVZ155316	-	MW390671	-	2

Taxon	Locality	Voucher Number	mt-Cytb	ifgb7	Ref. mt-Cytb	Ref. Ifgb7
O. delicatus	Venezuela: Sucre, Finca Vuelta Larga	AMNH257262	GU126529	MW390674	6	2
O. delicatus	Venezuela: Portuguesa, Hato Maporal near Caño Delgadito	TK138080	DQ227457	-	7	-
O. destructor destructor	Peru: Huánuco, Chinchao, Caserío de San Pedro de Carpish	MUSM19069	MG214280	MW390676	8	2
O. destructor spodiurus	Peru: Cajamarca, Chota, Querocoto	MUSM39519	MG214266	MW390675	8	2
O. flavescens	Brazil: São Paulo, Pedreira	CRB1430	JQ013746	JQ282855	9	9
O. flavescens	Uruguay: Maldonado, Barra Arroyo	GD729	MK128719	MW390678	1	2
O. fornesi	Argentina: Chaco, Parque Nacional Chaco	MACN22830	GU185920	-	4	-
O. fornesi	Argentina: Formosa, Colonia Buena Vista	INEVH36163	HQ890936	KY933614	10	Unp
O. fulvescens	Mexico: Tamaulipas, 5 km N of Soto La Marina	ROM96111	MK128743	MW390680	1	2
O. fulvescens	Honduras: Olancho, 4 km E Catacamas	TTU84699	MK128744	MW390679	1	2
O. guille	Peru: Ica, Pisco, Huamay, Pueblo Vernal, Lagunilla	MUSM26270	MK128702	MW390663	1	2

Taxon	Locality	Voucher Number	mt-Cytb	ifgb7	Ref. mt-Cytb	Ref. Ifgb7
O. guille	Peru: Ica, Pisco, Caucato	MUSM44245	MK128703	MW390664	1	2
O. longicaudatus	Argentina: Rio Negro, Bariloche	Bar23403	GU185912	KY933627	4	Unp
O. longicaudatus	Argentina: Neuquén	LB012	AY275702	-	11	-
O. longicaudatus	Chile	GD1198	-	MW390682	-	2
O. magellanicus	Chile: Magallanes	IPAT	AY275705	-	11	-
O. mattogrossae	Brazil: Mato Grosso do Sul, Corumbá	LBCE5718	KY952256	-	12	-
O. mattogrossae	Brazil: Bahia, Jaborandi	MN62640	KY952261	JQ282862	12	9
O. mattogrossae	Brazil: Mato Grosso, São José do Xingu, Fazenda São Luiz	CRB2793	-	PP395770	-	PS
O. mattogrossae	Brazil: Mato Grosso, São José do Xingu, Fazenda São Luiz	CRB2823	-	PP395771	-	PS
O. messorius	Venezuela: Amazonas, Pozon, 50 km NE of Puerto Ayacucho	ACUNHC275	EU258537	-	13	-

Taxon	Locality	Voucher Number	mt-Cytb	ifgb7	Ref. mt-Cytb	Ref. Ifgb7
O. messorius	Venezuela: Amazonas, Pozon, 50 km NE of Puerto Ayacucho	ROM107871	MK128745	MW390683	1	2
O. moojeni	Brazil: Goiás, Sitio D Abadia	LBCE11615	JQ013771	JQ282874	9	9
O. moojeni	Brazil: Goiás, Cavalcante	MN50309	JQ013768	JQ282844	9	9
O. nigripes	Brazil: Santa Catarina, Jaborá	LBCE8160	JQ013778	JQ282873	9	9
O. nigripes	Brazil: Rio de Janeiro, Parque Nacional da Serra dos Órgãos	MN71984/LBCE 6468	GQ259904	JQ282868	9	9
O. occidentalis	Bolivia: Cochabamba, 7.5 Km SE of Rodeo	MSB87148	MK128796	MW390689	1	2
O. occidentalis	Argentina: Salta	INEVH-Or22523	GU185914	-	4	-
O. occidentalis	Bolivia: Cochabamba, 28 km W Comarapa	MSB55318	-	MW390688	-	2
O. rupestris	Brazil: Goiás, Alto Paraiso	MN50322	JQ013763	JQ282850	9	9
O. rupestris	Brazil: Goiás, Alto Paraiso	MN50326	JQ013764	JQ282851	9	9
O. stramineus	Brazil: Goiás, Terezina de Goiás	MN46410	JQ013747	-	9	-

Taxon	Locality	Voucher Number	mt-Cytb	ifgb7	Ref. mt-Cytb	Ref. Ifgb7
O. stramineus	Brazil: Bahia, Palmeiras, Fazenda Alto Coités	MN84348/MW303	MF696155	OR651755	14	PS
O. stramineus	Brazil: Goiás, Terezina de Goiás	MN34439	-	JQ282842	-	9
O. utiaritensis	Brazil: Mato Grosso, Campo Novo do Parecis	MN75622	JQ013756	JQ282891	9	9
O. utiaritensis	Brazil: Mato Grosso, Campo Novo do Parecis	MN75625	JQ013752	JQ282893	9	9
O. vegetus	Costa Rica: Cartago, Volcan Irazu	ROM113156/F48462	EU258541	MW390691	13	2
O. vegetus	Costa Rica: Punta Arenas, Cerro Amigo	KU142065	EU192165	-	15	-
Oligoryzomys sp. n. Central clade	Brazil: Mato Grosso, Aripuanã	CIT683	OR651742	-	PS	-
Oligoryzomys sp. n. Central clade	Brazil: Rondônia, Alto Paraiso	AN693269	JX443659	-	16	-
Oligoryzomys sp. n. Central clade	Brazil: Rondônia, Alto Paraiso	AN693307	JX443657	-	16	-

Taxon	Locality	Voucher Number	mt-Cytb	ifgb7	Ref. mt-Cytb	Ref. Ifgb7
Oligoryzomys sp. n. Central clade	Brazil: Rondônia, Alto Paraíso	MN91084/LBCE 7038	OR651743	OR651754	PS	PS
Oligoryzomys sp. n. Central clade	Brazil: Rondônia, Alto Paraíso	MN91085/LBCE 7039	OR651744	-	PS	-
Oligoryzomys sp. n. Central clade	Brazil: Rondônia, Alto Paraiso, Faz. Seu Bento	LBCE20448/SVS 021	-	OR651749	-	PS
Oligoryzomys sp. n. Central clade	Brazil: Rondônia, Alto Paraiso, Faz. Seu Bento	LBCE20474/SVS 062	-	OR651750	-	PS
Oligoryzomys sp. n. Central clade	Brazil: Rondônia, Alto Paraiso, Faz. Seu Bento	LBCE20483/SVS 075	-	OR651751	-	PS
Oligoryzomys sp. n. Central clade	Brazil: Rondônia, Alto Paraiso, Faz. Seu Bento	LBCE20492/SVS 093	-	OR651752	-	PS
Oligoryzomys sp. n. Eastern clade	Brazil: Tocantins, Pium	UFES1442	HM594618	-	17	-

Taxon	Locality	Voucher Number	mt-Cytb	ifgb7	Ref. mt-Cytb	Ref. Ifgb7
Oligoryzomys sp. n. Eastern clade	Brazil: Tocantins, São Sebastião do Tocantins, Fazenda Osara II	MN81639/CRB1 448	KY952251	JQ282857	12	9
Oligoryzomys sp. n. Eastern clade	Brazil: Tocantins, São Sebastiao do Tocantins, Fazenda Osara II	MN76226/FO43	-	OR651753	-	PS
O. microtis	Bolivia: Santa Cruz	JMR68	MK128746	-	1	-
O. microtis	Bolivia, Santa Cruz, El Refugio	BYU19014	AY439000	-	18	-
O. microtis	Brazil: Acre, Capixaba	MN89725/SVS673	KY952263	-	12	-
O. microtis	Brazil: Acre, Capixaba	SVS676	KY952264	-	12	-
O. microtis	Brazil: Acre, Capixaba	SVS647	OR651745	-	PS	-
O. microtis	Brazil: Acre, Igarapé Porangaba	MVZ193785	U58381	-	19	-
O. microtis	Brazil: Acre, Porto Acre, Humaitá	MN87951/LBCE 18385	OR651746	-	PS	-

Taxon	Locality	Voucher Number	mt-Cytb	ifgb7	Ref. mt-Cytb	Ref. Ifgb7
O. microtis	Brazil: Acre, Porto Acre, Rodovia AC-10, Km 20, Ramal Profª Lucila	LBCE15126	OR651747	-	PS	-
O. microtis	Brazil: Acre, Rio Branco, Parque ZooBotânico	LBCE18400	OR651748	-	PS	-
O. microtis	Brazil: Amazonas, Itacoatiara	AN683313	JX443647	-	16	-
O. microtis	Brazil: Amazonas, Itacoatiara	AN683316	JX443648	-	16	-
O. microtis	Brazil: Amazonas, Itacoatiara	AN683318	JX443649	-	16	-
O. microtis	Brazil: Amazonas, Jainu, right bank Rio Juruá	MVZ193858	EU258549	MW390684	13	2
O. microtis	Brazil: Amazonas, Manacapuru	MN84349/CRB3004	KY952252	-	12	-
O. microtis	Brazil: Amazonas, Seringal Condor	MVZ190403	MK128748	-	1	-
O. microtis	Peru: Cusco	RCO468	MG988102	-	Unp	-
O. microtis	Peru: Loreto, Iquitos	TTU76247	MK128767	-	1	-
O. microtis	Peru: Loreto, Zona Marina	TTU76249	FJ374766	-	20	-
O. microtis	Peru: Madre de Dios, Puerto Maldonado	MUSM21839	MK128758	-	1	-

Taxon	Locality	Voucher Number	mt-Cytb	ifgb7	Ref. mt-Cytb	Ref. Ifgb7
O. microtis	Peru: Madre de Dios, Puerto Maldonado	MUSM21840	MK128759	-	1	-
O. microtis	Peru: Madre de Dios, Puerto Maldonado	MUSM21841	MK128760	-	1	-
O. microtis	Peru: Madre de Dios, Puerto Maldonado	MUSM21843	MK128762	-	1	-
O. microtis	Peru: Madre de Dios, Puerto Maldonado	MUSM21846	MK128765	MW390685	1	2
O. microtis	Peru: Loreto	MUSM43213	MG824921	-	Unp	-
OUTGROUPS						
Abrothrix longipilis	Chile, Aysen	NK160649	GU564074	GU564103	21	21
Thomasomys aureus	Peru, Cusco	MVZ170076	U03540	KJ614620	23	22
Sigmodon hispidus	Mexico, Tamaulipas	TK137315	EU073177	EU652895	24	24
Handleyomys saturatior	Nicaragua, Matagalpa	CURN JAGE438	KF658386	KF658445	26	26
Hylaeamys megacephalus	Brazil, Goiás	LBCE18571	KP122250	-	25	-

Taxon	Locality	Voucher Number	mt-Cytb	ifgb7	Ref. mt-Cytb	Ref. Ifgb7
Hylaeamys megacephalus	Brazil, Brasília	UNB3069	-	JQ966815	-	27
Lundomys molitor	Brazil, Rio Grande do Sul	MCNU2302	JQ966241	JQ966825	27	27
Melanomys chrysomelas	Nicaragua, Atlantico Norte	TK121417	EU340017	KP970194	28	28
Neacomys paracou	Suriname: Brokopondo, Brownsberg Nature Park, Headquarters	ROM114023	KP778425	KP778752	Unp	Unp
Oecomys auyantepui	Brazil: Pará, Óbidos	MPEG40457	OM927735	OM927739	29	29
Oryzomys couesi	Honduras, Olancho	TK102040	DQ185383	EU652903	7	24
Pseudoryzomys simplex	Argentina, Chaco	CNP4589	KP970127	KP970198	28	28
Sooretamys angouya	Paraguay, Ñeembucu	TK61763	KP970128	KP970200	28	28

Appendix 3. Haplotypes (H) of *O. microtis* and *Oligoryzomys* sp. n.. Numbers after localities refer to collecting sites in the map (fig. 1) Museum and collector acronyms are as in appendix 2. Brazilian states are Acre (AC), Amazonas (AM), Rondônia (RO), Tocantins (TO).

H	Taxon	Voucher	mt-Cytb	Locality	Ref.
1	*O. microtis*	MUSM43190	MG824919	Peru: Loreto	Unpublished. GenBank
1	*O. microtis*	MUSM43210	MG824922	Peru: Loreto	Unpublished. GenBank
1	*O. microtis*	MUSM43213	MG824921	Peru: Loreto	Unpublished. GenBank
1	*O. microtis*	MUSM43223	MG824920	Peru: Loreto	Unpublished. GenBank
2	*O. microtis*	MVZ193785	U58381	Brazil: AC, Igarapé Porangaba - 31	Patton and Silva 1995
3	*O. microtis*	MN87950/LBCE18369	OR709690	Brazil: AC, Porto Acre, Humaitá - 19	Present study
3	*O. microtis*	MN87951/LBCE18385	OR651746	Brazil: AC, Porto Acre, Humaitá - 19	Present study
3	*O. microtis*	LBCE15123	OR709691	Brazil: AC, Porto Acre, Rodovia AC-10, Km 20, Ramal Profª Lucila - 20	Present study
3	*O. microtis*	LBCE15135	OR709692	Brazil: AC, Porto Acre, Rodovia AC-10, Km 20, Ramal Profª Lucila - 20	Present study
3	*O. microtis*	LBCE15141	OR709693	Brazil: AC, Porto Acre, Rodovia AC-10, Km 20, Ramal Profª Lucila - 20	Present study
4	*O. microtis*	MUSM21839	MK128758	Peru: Madre de Dios, Puerto Maldonado - 23	Hurtado and D'Elía 2019
5	*O. microtis*	MN87930/SVS665	OR709694	Brazil: AC, Capixaba - 18	Present study
5	*O. microtis*	MUSM21841	MK128760	Peru: Madre de Dios, Puerto Maldonado -23	Hurtado and D'Elía 2019
5	*O. microtis*	MUSM21842	MK128761	Peru: Madre de Dios, Puerto Maldonado - 23	Hurtado and D'Elía 2019

5	*O. microtis*	MUSM21845	MK128764	Peru: Madre de Dios, Puerto Maldonado - 23	Hurtado and D'Elía 2019
6	*O. microtis*	AN683313	JX443647	Brazil: AM, Itacoatiara - 39	Firth et al. 2012
7	*O. microtis*	AVG711	MG988103	Peru: Cusco, La Convencion, Echarate - 41	Unpublished. GenBank
7	*O. microtis*	RCO468	MG988102	Peru: Cusco	Unpublished. GenBank
8	*O. microtis*	AN683316	JX443648	Brazil: AM, Itacoatiara - 39	Firth et al. 2012
9	*O. microtis*	MVZ190401	HM594624	Brazil: AM, Seringal Condor - 33	Rocha et al. 2011
9	*O. microtis*	MVZ190403	MK128748	Brazil: AM, Seringal Condor - 33	Hurtado and D'Elía 2019
10	*O. microtis*	MVZ193858	EU258549	Brazil: AM, Jainu - 32	Rogers et al. 2009
11	*O. microtis*	SVS647	OR651745	Brazil: AC, Capixaba - 18	Present study
12	*O. microtis*	MN84349/CRB3004	KY952252	Brazil: AM, Manacapuru - 22	Weksler et al. 2017
13	*O. microtis*	MUSM21843	MK128762	Peru: Madre de Dios, Puerto Maldonado -23	Hurtado and D'Elía 2019
13	*O. microtis*	MUSM21844	MK128763	Peru: Madre de Dios, Puerto Maldonado - 23	Hurtado and D'Elía 2019
14	*O. microtis*	TTU76247	MK128767	Peru: Loreto, Iquitos - 42	Hurtado and D'Elía 2019
14	*O. microtis*	TTU76248	MK128768	Peru: Loreto, Iquitos - 42	Hurtado and D'Elía 2019
15	*O. microtis*	TTU76249	FJ374766 = MK128766	Peru: Loreto, Iquitos - 42	Richter et al. 2010; Hurtado and D'Elía 2019
16	*O. microtis*	JMR68	MK128746	Bolivia: Santa Cruz - 35	Hurtado and D'Elía 2019
17	*O. microtis*	BYU19014	AY439000	Bolivia: Santa Cruz, los Mineros, Dinamarca - 36	Carroll et al. 2005

18	*O. microtis*	LBCE15126	OR651747	Brazil: AC, Porto Acre, Rodovia AC-10, Km 20, Ramal Profª Lucila - 20	Present study
19	*O. microtis*	MUSM21840	MK128759	Peru: Madre de Dios, Puerto Maldonado - 23	Hurtado and D'Elía 2019
20	*O. microtis*	SVS676	KY952264	Brazil: AC, Capixaba - 18	Weksler et al. 2017
21	*O. microtis*	LBCE13098	OR709695	Brazil: AC, Brasiléia - 17	Present study
21	*O. microtis*	MN97925/SVS642	OR709696	Brazil: AC, Capixaba - 18	Present study
21	*O. microtis*	MUSM21846	MK128765	Peru: Madre de Dios, Puerto Maldonado	Hurtado and D'Elía 2019
22	*O. microtis*	MN97923/SVS639	OR709697	Brazil: AC, Capixaba - 18	Present study
22	*O. microtis*	MN97924/SVS641	OR709698	Brazil: AC, Capixaba - 18	Present study
22	*O. microtis*	MN97926/SVS643	OR709699	Brazil: AC, Capixaba - 18	Present study
22	*O. microtis*	MN97927/SVS645	OR709700	Brazil: AC, Capixaba - 18	Present study
22	*O. microtis*	MN87929/SVS663	OR709701	Brazil: AC, Capixaba - 18	Present study
22	*O. microtis*	MN87931/SVS666	OR709702	Brazil: AC, Capixaba - 18	Present study
22	*O. microtis*	SVS712	OR709703	Brazil: AC, Capixaba - 18	Present study
22	*O. microtis*	MN87952/LBCE18400	LBCE18400	Brazil: AC, Rio Branco, Parque ZooBotânico - 21	Present study
23	*Oligoryzomys* sp. n. Central clade	AN693262	JX443656	Brazil: RO, Alto Paraiso - 7	Firth et al. 2012
23	*Oligoryzomys* sp. n. Central	SVS106	OR709704	Brazil: RO, Alto Paraíso - 7	Present study

	clade				
23	*Oligoryzomys* sp. n. Central clade	MN91085/LBCE7039	OR651744	Brazil: RO, Alto Paraíso - 7	Present study
24	*Oligoryzomys* sp. n. Central clade	AN693269	JX443659	Brazil: RO, Alto Paraiso - 7	Firth et al. 2012
25	*Oligoryzomys* sp. n. Central clade	AN693231	JX443651	Brazil: RO, Alto Paraiso - 7	Firth et al. 2012
25	*Oligoryzomys* sp. n. Central clade	AN693239	JX443652	Brazil: RO, Alto Paraiso - 7	Firth et al. 2012
25	*Oligoryzomys* sp. n. Central clade	AN693240	JX443660	Brazil: RO, Alto Paraiso - 7	Firth et al. 2012
25	*Oligoryzomys* sp. n. Central clade	AN693244	JX443653	Brazil: RO, Alto Paraiso - 7	Firth et al. 2012
25	*Oligoryzomys* sp. n. Central clade	AN693251	JX443654	Brazil: RO, Alto Paraiso - 7	Firth et al. 2012
25	*Oligoryzomys* sp. n. Central clade	AN693277	JX443661	Brazil: RO, Alto Paraiso - 7	Firth et al. 2012
25	*Oligoryzomys* sp. n. Central clade	AN693288	JX443662	Brazil: RO, Alto Paraiso - 7	Firth et al. 2012
25	*Oligoryzomys* sp. n. Central clade	AN693292	JX443663	Brazil: RO, Alto Paraiso - 7	Firth et al. 2012
25	*Oligoryzomys* sp. n. Central clade	AN693338	JX443658	Brazil: RO, Alto Paraiso - 7	Firth et al. 2012

25	*Oligoryzomys* sp. n. Central clade	MN91084/LBCE7038	OR651743	Brazil: RO, Alto Paraíso - 7	Present study
25	*Oligoryzomys* sp. n. Central clade	MN87919/SVS118	OR709705	Brazil: RO, Alto Paraíso - 7	Present study
25	*Oligoryzomys* sp. n. Central clade	MN87921/SVS134	OR709706	Brazil: RO, Alto Paraíso - 7	Present study
26	*Oligoryzomys* sp. n. Eastern clade	MN81639/CRB1448	KY952251	Brazil: TO, São Sebastião do Tocantins - 8	Weksler et al. 2017
27	*Oligoryzomys* sp. n. Eastern clade	UFES1442	HM594618	Brazil: TO, Pium - 11	Rocha et al. 2011

Appendix 4. Vector correlation loadings of principal components (PC1, PC2, PC3), coefficients of canonical discriminant functions (DF1 and DF2), and percentage of variation for multivariate analysis of selected samples of the *Oligoryzomys microtis*.

Variable	PC1	PC2	PC3	DF1	DF2
CIL	0.80	-0.34	-0.06	-0.27	-0.41
LD	0.27	-0.12	-0.03	-0.49	-0.19
PB	0.14	-0.17	-0.59	0.45	-0.75
LIF	0.13	-0.25	0.31	0.45	0.18
BIF	0.04	-0.12	-0.03	0.58	-0.21
LM	0.03	0.12	-0.32	-0.49	-0.33
BM1	0.02	0.03	-0.03	0.72	0.10
M1M	0.09	0.17	-0.06	-0.73	-0.10
BRO	0.16	-0.02	-0.03	-0.32	-0.12
ORL	0.27	0.17	0.65	0.58	0.42
ZB	0.37	0.83	-0.14	-0.28	0.62
BZP	0.07	0.00	0.01	0.10	0.58
Prop. Variance	77%	5%	4%	52%	48%
Cumulative Prop.	77%	83%	87%	52%	100%

HYSTRIX
the Italian Journal of Mammalogy

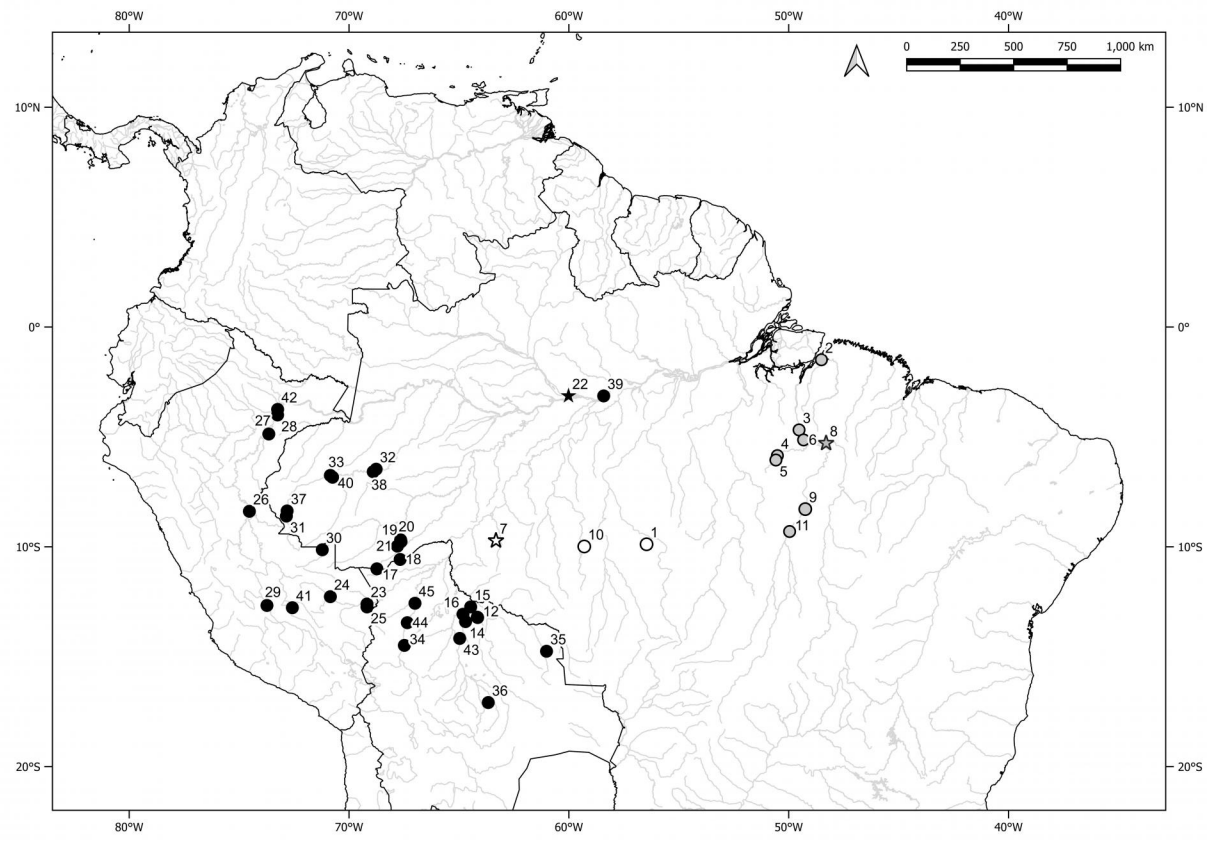

Figure 1. Map showing the collecting localities of O. microtis (black symbols), and Oligoryzomys sp. n. (grey and white symbols); starts correspond to type localities. Numbers refer to localities listed in appendices 1 and 2 and table 1.

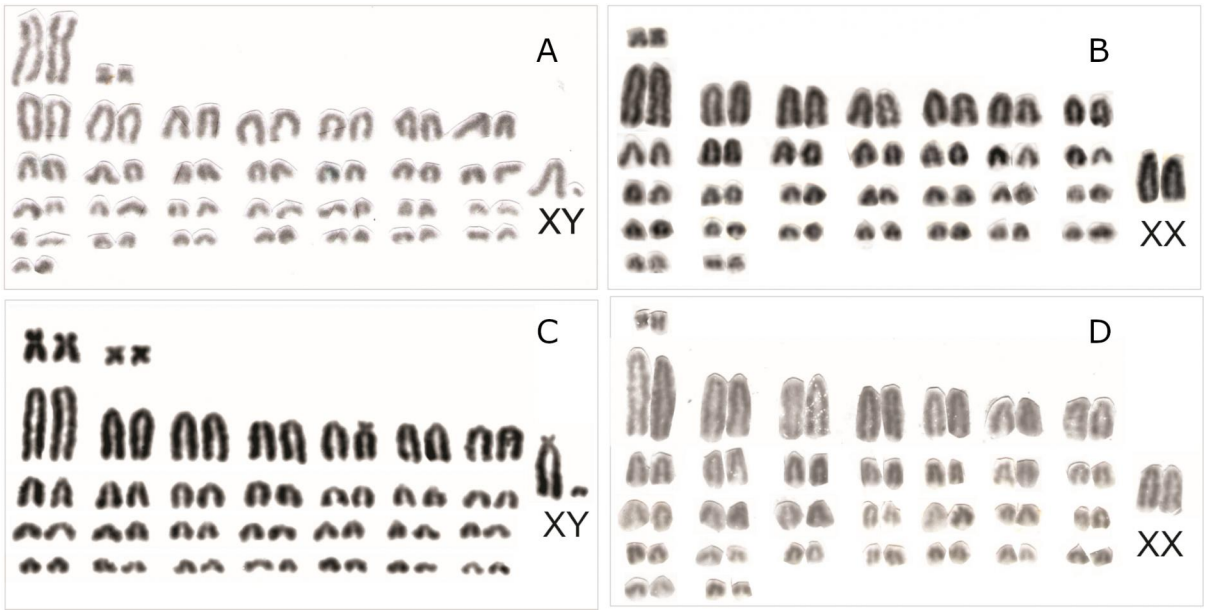

Figure 2. Karyotypes in conventional coloration of (A) O microtis topotype male MN84349 with 2n=64 and FN=66, (B) Oligoryzomys sp. n. female MN91085 from Central clade (Rondônia, Brazil), with 2n=64 and FN=64, (C) O. mattogrossae male CRB3141 from Brasília, Brazil with 2n=62 and FN=64, and (D) Oligoryzomys sp. n. female MN81643 from Eastern clade (Tocantins, Brazil) with 2n=64 and FN=64.

HYSTRIX
the Italian Journal of Mammalogy

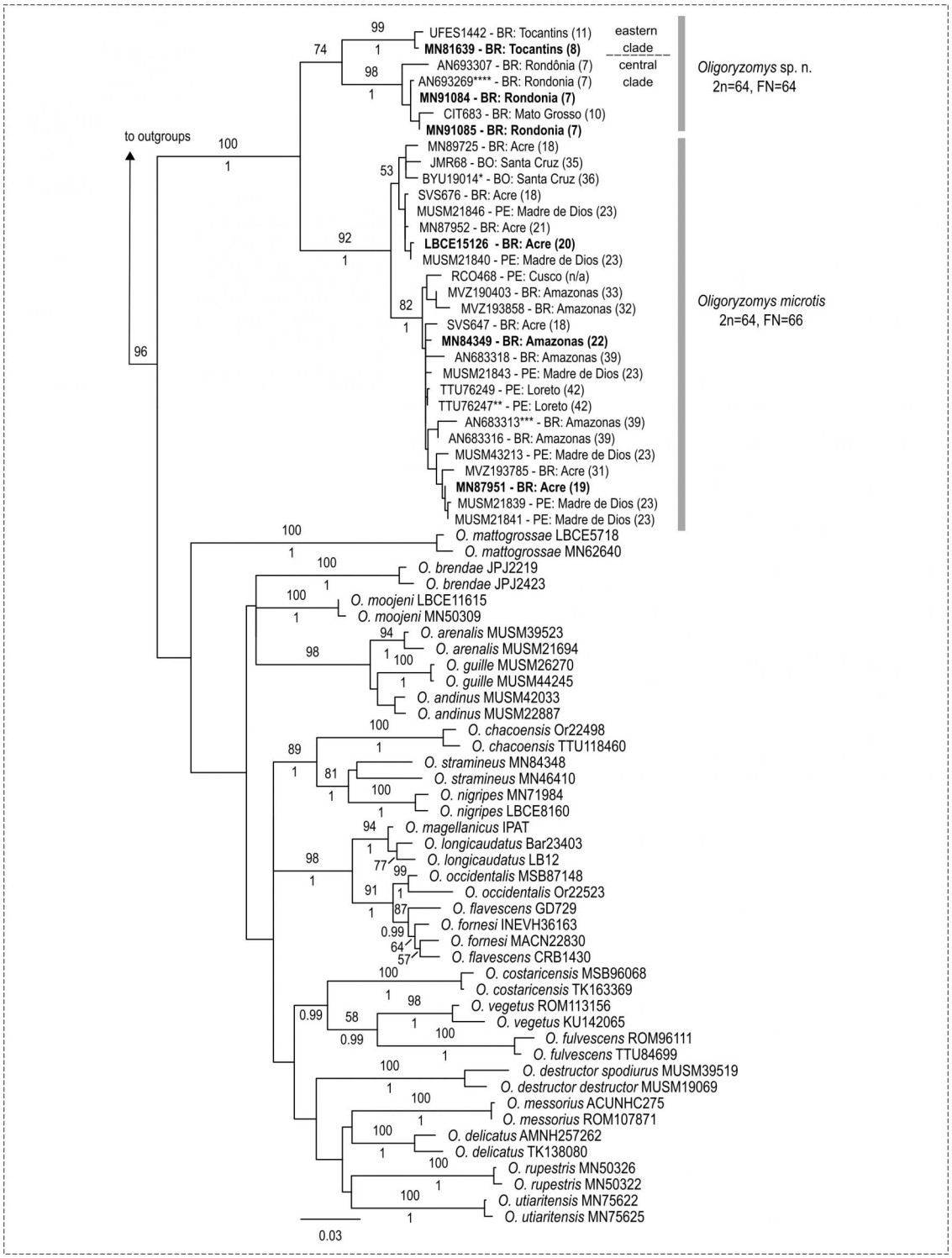

Figure 3. Phylogenetic relationships among Oligoryzomys specimens based on maximum likelihood analyses of mt-Cytb. Bootstrap values (bs, %) are shown above branches; posterior probabilities of Bayesian analysis are shown below branches. Locality numbers for O. microtis and Oligoryzomys sp. n. are in parentheses; diploid number (2n) and fundamental number (FN) are based on karyotyped specimens marked in bold; specimens that were reported positive for virus-specific RNA hantavirus are marked with asterisks: * for RIOMV strain (Bharadwaj et al. 1997; Carroll et al. 2005); ** for strain HTN-007 (Powers et al. 1999; Oliveira et al. 2014); *** for RIOMV-3 (Firth et al. 2012); and **** for RIOMV-4 (Firth et al. 2012). See appendix 2 for outgroups and specimen information.

HYSTRIX
the Italian Journal of Mammalogy

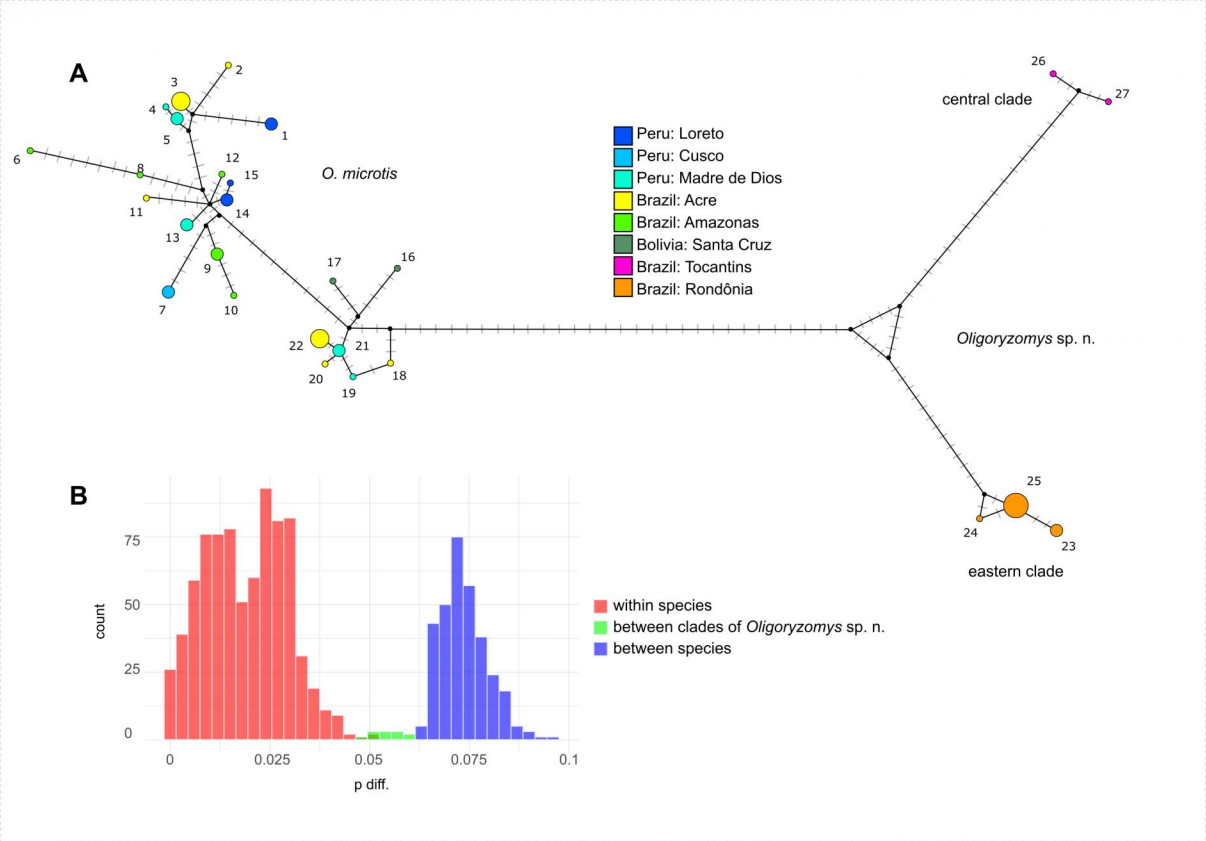

Figure 4. (A) Median joining network with O. microtis and Oligoryzomys sp. n.. Circles are haplotypes proportional to number of shared sequences; small black circles are median vectors; small bars indicate nucleotide substitutions; numbers refer to haplotype numbers listed in appendix 3; see legend for geographic source of haplotypes. (B) Pairwise uncorrected (´p´) genetic distances for 3 contrasts: within species, between clades of Oligoryzomys sp. n. and between species.

HYSTRIX
the Italian Journal of Mammalogy

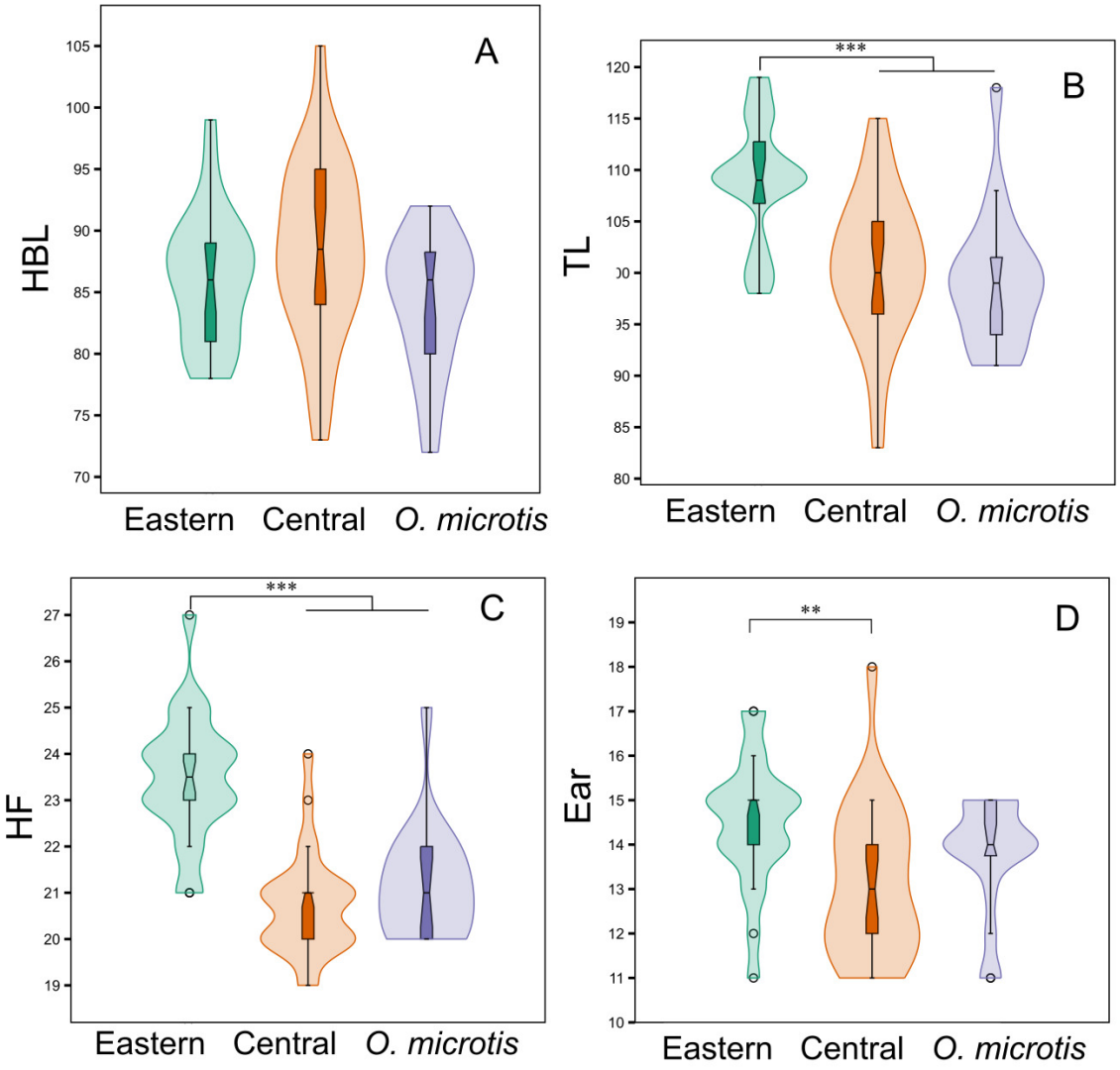

Figure 5. Combined violin plot with box plot for external measurements for E of Oligoryzomys microtis complex. Violin plot shows kernel density plot from minimum to maximum value. The box plot shows the median, 25-75 percent quartiles (boxes), values less or more than 1.5 times the box height (whiskers), and outliers. Measurements are: (A) HBL: head-and-body length, (B) TL: tail length, (C) HF: hind-feet length, and (D) Ear: ear length. Lines above each graph show significant differences among groups: ** < 0.01, *** < 0.001.

Figure 6. Dorsal, lateral and ventral views of skins of Oligoryzomys sp. n. from Eastern Clade (Tocantins State, MN76206), Oligoryzomys sp. n. from Central Clade (Rondônia State, MN87921), and O. microtis (Acre State, MN87929).

HYSTRIX
the Italian Journal of Mammalogy

Figure 7. Dorsal, ventral, and lateral views of the skull of Oligoryzomys sp. n. from Central clade (Rondônia State, MN87921), Oligoryzomys sp. n. from Eastern Clade (Tocantins State, MN76206).

HYSTRIX
the Italian Journal of Mammalogy

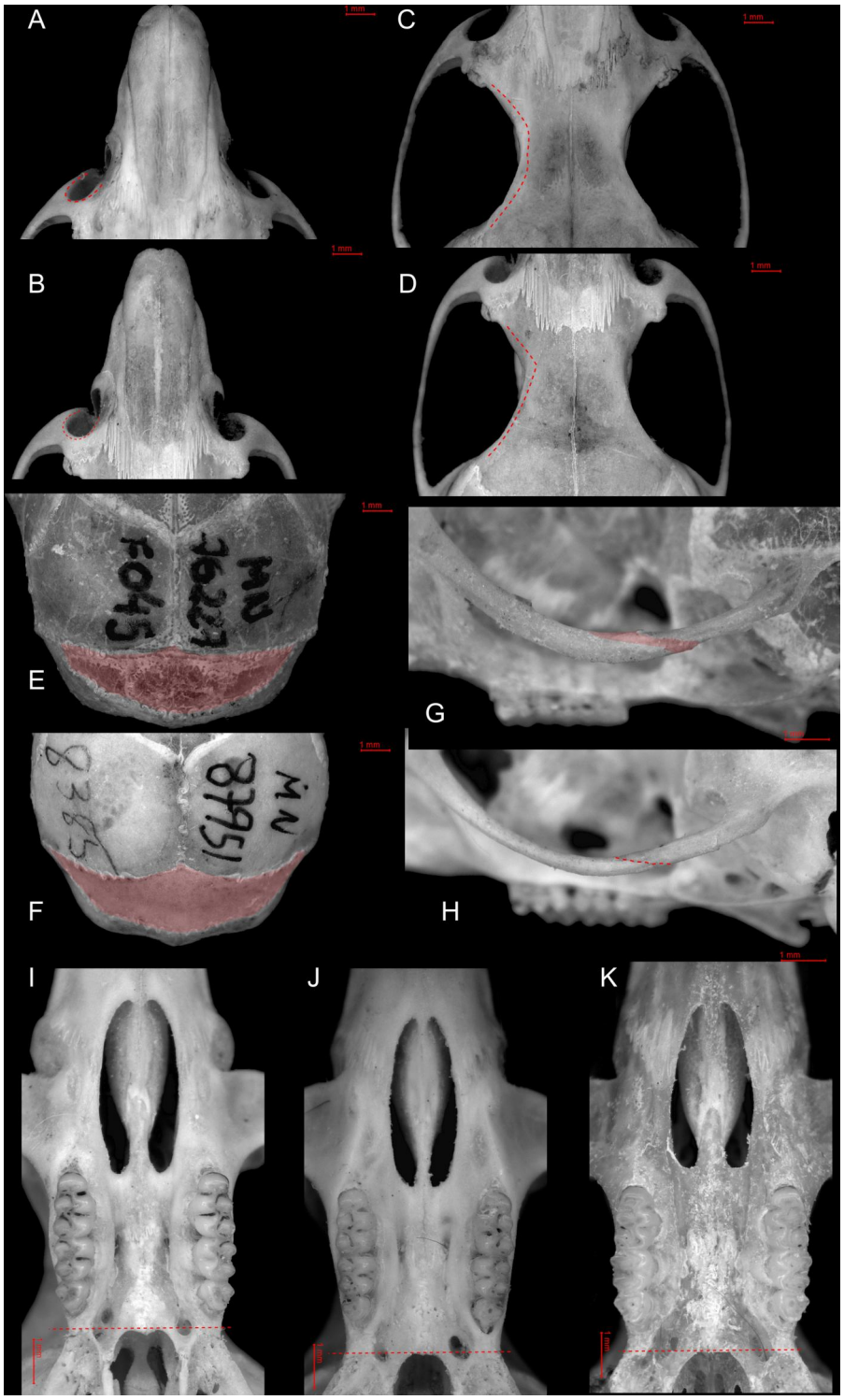

Figure 8. Comparative plate of Oligoryzomys skulls, showing the variation of six selected qualitative traits: depth of the zygomatic notch (dorsal view; A-B), interorbital region (dorsal view, C-D), width of interparietal (dorsal view, E-F), presence of jugal (lateral view; G-H), and shape of incisive foramina and length of palate (ventral view; I-K). (A) Oligoryzomys sp. n., central clade (MN87906); (B, D, F, H, I) O. microtis (MN87951); (C) Oligoryzomys sp. n., central clade (MN87901); (E, G, K) Oligoryzomys sp. n., eastern clade (MN76227); (J) Oligoryzomys sp. n., central clade (MN87907).

HYSTRIX
the Italian Journal of Mammalogy

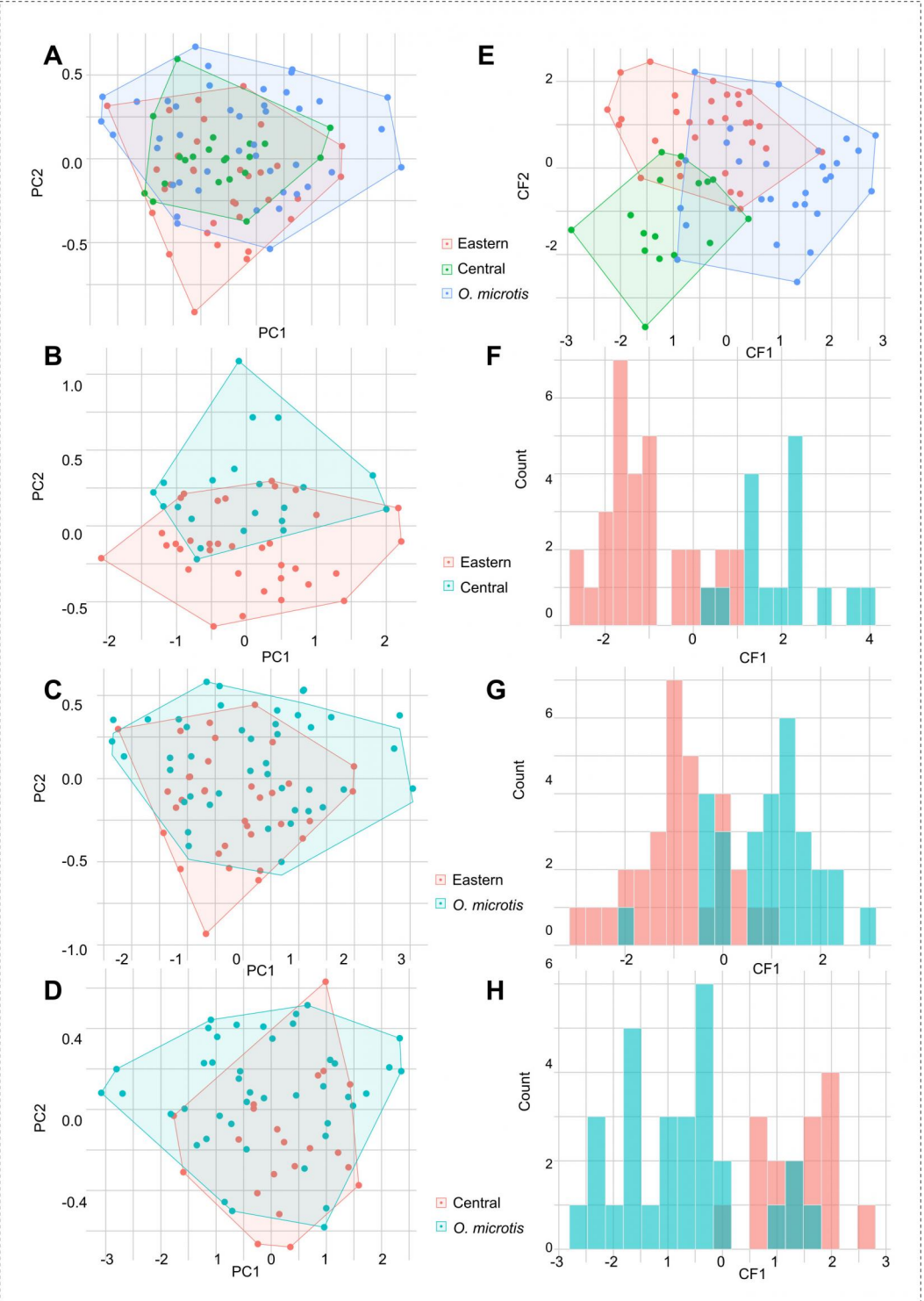

Figure 9. Results of principal component analysis (A-D) and canonical discriminant analysis (E-H) of log-transformed cranial measurements. Scatterplots A and E include all analyzed specimens, while remaining graphs refer to pairwise contrasts between: (B and F) eastern and central clades of Oligoryzomys sp. n., (C and G) O. microtis and eastern clade of Oligoryzomys sp. n., and (D and H) O. microtis and central clade of Oligoryzomys sp. n..